Estimation of Mechanical and Hydraulic Parameters of Bentonite-Soil Mixtures in Oedometer Condition with Index Properties

An LI
Department of Civil and Environmental Engineering
The Hong Kong Polytechnic University, Hong Kong, China
Email: an0929.li@connect.polyu.hk

Wen-Bo CHEN
Department of Civil and Environmental Engineering
The Hong Kong Polytechnic University, Hong Kong, China
Email: geocwb@gmail.com
wb.chen@polyu.edu.hk

Ze-Jian CHEN
Department of Civil and Environmental Engineering
The Hong Kong Polytechnic University, Hong Kong, China
Email: ze-jian.chen@connect.polyu.hk

Pei-Chen WU
Department of Civil and Environmental Engineering
The Hong Kong Polytechnic University, Hong Kong, China
Email: elvis.wu@polyu.edu.hk

Jian-Hua YIN[1,2]
1: Department of Civil and Environmental Engineering
2: Research Institute for Land and Space
The Hong Kong Polytechnic University, Hong Kong, China
Email: cejhyin@polyu.edu.hk

And

Chao ZHOU
Department of Civil and Environmental Engineering
The Hong Kong Polytechnic University, Hong Kong, China
Email: c.zhou@polyu.edu.hk

Abstract

A large amount of bentonite slurry is dumped as construction waste in fill banks around the world. In order to reuse them, it is important to determine the mechanical and hydraulic parameters of bentonite-soil mixtures containing different montmorillonite contents. The establishment of these parameters with index properties is an efficient and simple way. Despite the proposal of some correlations to estimate the compression and swelling indices for kaolinite or illite-dominated soils (KIDSs) with relatively low liquid limits, they are unsuitable for bentonite-soil mixtures dominated by montmorillonite. Besides, no correlation was given for predicting the parameters in the non-linear creep function as well. In this study, the results of the index, oedometer and scanning electron microscope (SEM) tests on five mixtures with different montmorillonite contents from 5% to 35% were presented. Compression and swelling indices creep coefficient as well as the non-linear creep parameters and hydraulic conductivity of bentonite-soil mixtures were obtained. Several correlations were put forward to estimate the mechanical parameters with Atterberg limit indices. The proposed correlations were further verified using the data collected from literature, which can well estimate the mechanical parameters of soils with a liquid limit of above 50%. In addition, a simplified model with a homogenization approach was developed to estimate hydraulic conductivity, which is easier to be adopted in practical engineering.

Keywords: **Bentonite Slurry; Montmorillonite Content; Correlation; Homogenization; Mixture**

Introduction

Bentonite is commonly used in civil engineering, including the construction of diaphragm walls, the operation of tunnel boring machines, etc. However, the used bentonite slurry is a kind of construction waste that might pollute water and soil. It is challenging to dispose of massive bentonite slurry all over the world. When economic, environmental and sustainable development factors are taken into account, the used bentonite slurry shall be dewatered before being moved and disposed of as fill material at a permanent disposal site or consolidated in situ with additional fills to provide land for other developments. If bentonite slurry is used as fill material to support any structure, its hydraulic conductivity (k), compressibility, long-term behavior and corresponding mechanical parameters such as creep coefficient ($C_{\alpha e}$) and compression (C_c) and swelling indices (C_s) are important in the design of geotechnical applications. These parameters must be determined in advance. Nevertheless, bentonite slurry generally contains different montmorillonite contents ranging from 4% to 40% due to the different dosages of bentonite in different projects (Amarasinghe et al., 2012). Oedometer tests require high-quality undisturbed soil specimens which are quite expensive and time-consuming, especially with the incorporation of the creep stage (Yin, 1999b). In terms of time and cost, it is infeasible to conduct oedometer tests on all undisturbed soil specimens with different clay contents (Zhang et al., 2021). Establishing correlations with index properties could provide the preliminarily estimated values of soil parameters for practical engineering design.

To overcome the above-mentioned inconvenience, some attempts have been made to establish correlations between mechanical parameters and index properties (e.g., liquid limit, plasticity index or void ratio at the liquid limit) for soils since it is much easier to obtain the indices of soils in the laboratory. Proposed by Skempton (1944), the first correlation with the liquid limit (w_L) for predicting compression index is one of the most widely used correlations at present. In the following decades, extensive attempts have been made to correlate compression index with a variety of physical parameters, including liquid limit (Terzaghi & Peck, 1948; Cozzolino, 1961; Yin, 1999b), plasticity index, I_P (Wroth & Wood, 1978; Nakase et al., 1988; Tiwari & Ajmera, 2012) and void ratio at liquid limit e_L (Nagaraj & Murthy, 1983; Burland, 1990). Nonetheless, no correlation can perfectly predict the compression index with different property indices for all kinds of soil owing to the variation in the type and localization of different soils (Verbrugge & Schroeder, 2018).

Bentonite also exhibits obvious swelling behavior because of particle surface hydration and exchangeable cations as well as osmosis with electrical double-layer repulsion (Oscarson et al., 1990; Sridharan, 1999; Yilmaz & Marschalko, 2014; Yin et al., 2021). Therefore, the swelling index is also rather necessary in the geotechnical design for bentonite-soil mixtures since the swelling behavior of mixtures may lead to unexpected differential settlement. Previous research has correlated the swelling index with different index properties (Nakase et al., 1988; Yin, 1999b; Tiwari & Ajmera, 2011). Some researchers tried to make use of artificial neural networks to predict the swelling index (Kordnaeij et al., 2015; Kurnaz et al., 2016), whereas no previous research focused on bentonite mixtures with strong swelling properties. Thus, the establishment of the swelling index with liquid limit, plasticity index or other geotechnical properties for bentonite mixtures is needed.

Some attempts have been made for estimating hydraulic conductivity (Pandian et al., 1995; Sivapullaiah et al., 2000; Chapuis, 2012; Deng et al., 2017). A majority of equations are on the basis of the relationship between hydraulic conductivity and the e_L/e_0 value. Shi and Yin (2018) put forward a theoretical model based on the homogenization approach to predict the hydraulic conductivity of marine clay-sand mixtures with different sand contents. The theoretical model can still be greatly simplified despite being able to well predict the hydraulic conductivity of binary mixtures.

In general, clayey soils demonstrate creep behavior under laboratory and in situ conditions during both primary and secondary consolidation (Yin & Graham, 1989; Feng et al., 2017) owing to viscosity significantly affecting the long-term settlement of reclamation lands or other soft soil foundations. The creep coefficient must be determined beforehand in the long-term settlement calculation for both engineering practice and constitutive modeling incorporating viscous characteristics. As stated before, however, it takes more time to measure the creep coefficient in oedometer tests. Several correlations have been proposed for the preliminary estimation of the creep coefficient (Nakase et al., 1988; Yin, 1999b; Zeng et al., 2012; Yin et al., 2014; Zhu et al., 2016). Yin (1999a) pointed out that the use of the logarithmic function overestimates creep settlement due to the non-linearity of soil creep behavior, and thus proposed a function to fit the nonlinear creep behavior of soils. Correlating these nonlinear parameters with easily obtained geotechnical indexes could be meaningful for the application in practical engineering in that solving the nonlinear creep function is somewhat complicated for practical use.

The correlations proposed in the literature are summarized in Table 1, which can only be capable of predicting one or more specific kinds of soil. Most of them mainly focus on kaolinite or illite-dominated soils (KIDSs), thereby indicating their inability to predict the parameters of soils with high liquid limits or plasticity index, particularly montmorillonite-dominated soils (MDSs). It can be also found that no relevant correlation remains available in the literature for estimating nonlinear creep parameters. Meanwhile, it is also necessary to achieve the estimation of hydraulic conductivity easily. Hence, new correlations for estimating mechanical parameters and a model with a homogenization approach should be proposed to better understand the relationships between the mechanical parameters and Atterberg limit indices of montmorillonite-soil mixtures.

Table 1 Correlations of C_c, C_s and $C_{\alpha e}$ available in the literature

Correlation	Applicability	Reference
$C_c = 0.007(w_L - 10)$	Remoulded clays	Skempton (1944)
$C_c = 0.009(w_L - 10)$	Normally consolidated clays	Terzaghi and Peck (1967)
$C_c = 0.0046(w_L - 9)$	Brazilian clays	Cozzolino (1961)
$C_c = 0.0102w_L - 0.131$	Hong Kong Marine Deposit (HKMD)	Yin (1999)
$C_c = 0.0012w_L$	Remoulded clays with activity >1	Tiwari and Ajmera (2012)
$C_c = 0.0104I_p + 0.046$	Kawasaki clay and natural marine clay	Nakase *et al.* (1988)
$C_c = 0.0138I_p + 0.00732$	HKMD	Yin (1999)
$C_c = 0.75(e_0 - 0.5)$	Soils with low plasticity	Sowers (1970)
$C_c = 0.2237e_L$	Remoulded normally consolidated clay	Nagaraj and Murthy (1983)
$C_c = 0.208e_0 + 0.0083$	Chicago clays	Bowles (1989)
$C_c = 0.3921e_L$	Remoulded clays with activity >1	Tiwari and Ajmera (2012)
$C_s = 0.0007w_L + 0.0062$	Fine grained soils	Sinan (2009)
$C_s = 7\times10^{-6}\times(w_L)^2 - 0.0014w_L$	Remoulded montmorillonite -sand mixtures	Tiwari and Ajmera (2011)

$C_s = 0.00194 I_p - 0.00892$	Kawasaki and natural marine clays	Nakase *et al.* (1988)
$C_s = 0.00219 I_p - 0.0104$	HKMD	Yin (1999)
$C_s = 6 \times 10^{-6} \times (I_p)^2 - 0.0026 I_p$	Remoulded montmorillonite -sand mixtures	Tiwari and Ajmera (2011)
$C_s = 0.015(e_0 + 0.007)$	Clays with w_L>100%	Azzouz *et al.* (1976)
$C_s = 0.0087(e_0)^2 + 0.031 e_0$	Remoulded montmorillonite -sand mixtures	Tiwari and Ajmera (2011)
$C_{\alpha e} = 0.00033 I_p + 0.00168$	Kawasaki and natural marine clays	Nakase *et al.* (1988)
$C_{\alpha e} = 0.000369 I_p - 0.00055$	HKMD	Yin (1999)

In the present study, a series of index and oedometer tests were performed on bentonite-soil mixtures. Based on the model established by Shi and Yin (2018), a simplified method with a homogenization approach was proposed for the estimation of hydraulic conductivity. Scanning electron microscope (SEM) analysis interpreted compressibility and homogenization from the micro perspective. Correlations for predicting the mechanical parameters of soils were derived from the results of oedometer tests. The correlations proposed in this paper were further verified with the data collected from the literature.

Materials and experiment procedures

In this study, a range of multi-stage loading (MSL) oedometer tests was conducted on the bentonite-soil mixtures which were made by mixing two materials. The first one is bentonite slurry originally collected from a disposal site in Hong Kong. Soils from 11 locations of different depths were mixed with an excavator in the field to obtain a more uniform sample. Comprising fine sand, silt and clay particles, this bentonite slurry is slightly dark grey. The other is a commercially available pure bentonite named Bentonil® GCT 4 and obtained from the company Clariant. As sodium bentonite in dark yellow, Bentonil® GCT 4 is extensively used in different civil engineering projects in Hong Kong. Quantitative X-ray diffraction (QXRD) tests were carried out on the two samples, to determine the mineralogical composition of the two materials and further mix them to specific montmorillonite content. The mineralogical composition of the two materials is shown in Table 2.

Table 2 Mineralogical composition of the two materials (Unit: wt%)

Sample	Montmorillonite	Quartz	Feldspar	Others
Bentonite slurry	4	49	11	36
Bentonil® GCT 4	84	4	5	7
BS-5%*	5	48	11	36
BS-15%*	15	43	10	32
BS-20%*	20	40	10	30
BS-25%*	25	37	10	28
BS-35%*	35	31	9	25

*The mineralogical composition of mixtures was calculated according to the XRD results of bentonite slurry and Bentonil® GCT 4

Five bentonite-soil mixtures with different montmorillonite contents were prepared in light of the QXRD results and named BS-5%, -15%, -20%, -25% and -35%, respectively. All specimens were physically characterized to determine their particle size distribution, liquid and plastic limits, plasticity index and initial void ratio in accordance with British Standard 1377 (2016) in the laboratory. The particle size distribution curves and basic properties of all five mixtures are illustrated in Fig. 1 and Table 3, respectively.

Table 3 Basic properties of bentonite-soil mixtures

	BS-5%	BS-15%	BS-20%	BS-25%	BS-35%	Bentonil® GCT 4
Liquid limit, w_L (%)	56	86	114	135	181	390
Plastic limit, w_P (%)	21	27	31	34	37	63
Plasticity index, I_P (%)	35	59	83	101	144	327

Prior to oedometer tests, the bentonite-soil mixtures with a water content of 1.4 times their liquid limit were poured into a cylindrical steel mould for self-weight consolidation. Then, a vertical pressure from 5 to 40 kPa was gradually applied to the slurry for one-dimensional pre-consolidation to obtain consistent soil specimens. Upon the completion of the pre-consolidation process under the maximum pressure of 40 kPa, five saturated bentonite mixture specimens with a diameter of 70 mm and a thickness of 19 mm were taken from the mould by the use of confining rings for all oedometer tests. Silicon grease was smeared on the inner wall of each confining ring in order to minimize the friction between the ring and the soil specimen. Additionally, filter papers were positioned on both the top and bottom surfaces of each specimen to prevent soil particles from entering porous stones.

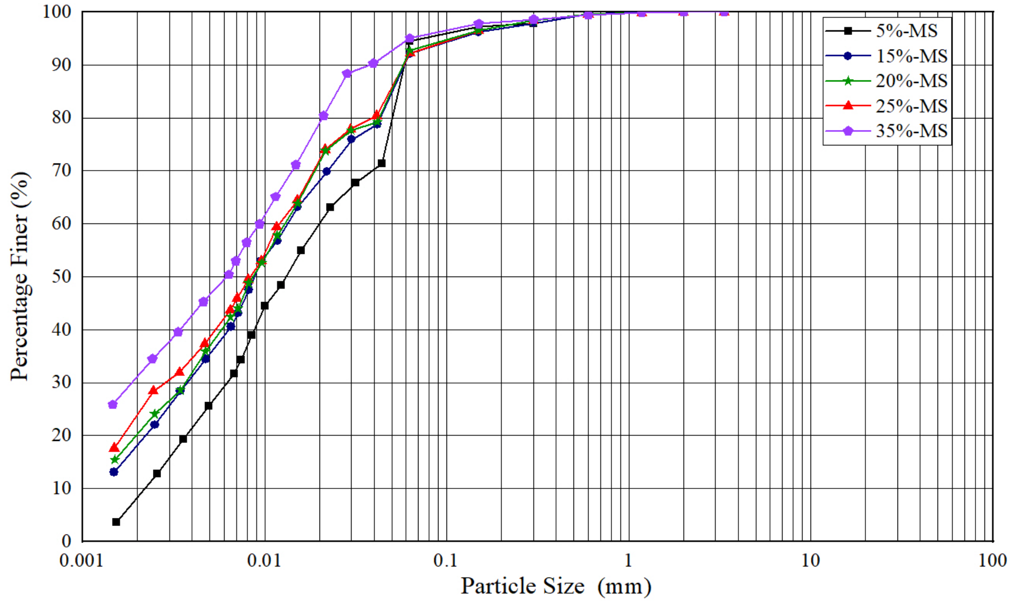

Fig. 1 Particle size distribution curves of bentonite-soil mixtures with different montmorillonite contents

MSL oedometer tests were carried out with Casagrande-type oedometers on the five bentonite-soil mixture specimens. The minimal consolidation stress of 5 kPa was applied instantly to reach equilibrium, followed by the consolidation of specimens with the subsequent instant loadings of 10, 20, 50, 100, 200 and 400 kPa. To get the swelling index C_s, the stress gradually decreased from 400 to 50 kPa and then reloaded to the final stress level of 800 kPa in the same incremental steps. Stages before 50 kPa and unloading-reloading stages lasted for 1,440 min. The rest of the stages were maintained for five days to ensure that all specimens had sufficient time to exhibit long-term creep behavior. MSL oedometer tests were also conducted on pure bentonite, namely Bentonil® GCT 4, to obtain its hydraulic conductivity for building a model with a homogenization approach. After oedometer tests, artificial bentonite-soil mixtures were dried by vacuum under -82 °C for 24h with a freeze dryer used for keeping the original microstructure. After that, the dry specimens were cut into cubes with sides of 6 mm for SEM observation.

Results and discussion

The results of oedometer tests conducted on bentonite-soil mixture specimens with different montmorillonite contents were presented and discussed. Particular emphasis was placed on the following aspects: (a) correlations of soil parameters (C_c, C_s and $C_{\alpha e}$) with Atterberg limit indices, (b) relationships between parameters (ψ_0' and ε_c^l) in the nonlinear function proposed by Yin (1999a) and basic indices, (c) a simplified model with a homogenization approach and (d) microfabric analysis.

Correlations of Atterberg limit indices

Liquid limit and plasticity index were determined in accordance with British Standard 1377 (2016) and summarized (see Table 3). Regarding the five artificial mixture specimens utilized in this study, their activity values defined as the ratio of plasticity index to clay content were found to be all greater than 1. Moreover, correlating the montmorillonite content and basic property indices of bentonite-soil mixtures could be extremely meaningful for practical engineering. As a result, Fig. 2 displays the three straight lines best fitting the montmorillonite content and the results of liquid and plastic limits as well as the plasticity index for all specimens as follows:

$$w_L = 4.259(MC + 6.865) \tag{1}$$

$$w_p = 0.59(MC + 33.57) \tag{2}$$

$$I_p = 3.699(MC + 2.82) \tag{3}$$

where MC denotes the montmorillonite content in percentage. As demonstrated in Fig. 2, the coefficients of determination (R^2) for the fitting lines of w_L, w_p and I_P are 0.986, 0.926 and 0.978, respectively. This means that strong correlations existed between montmorillonite content and liquid and plastic limits as well as the plasticity index.

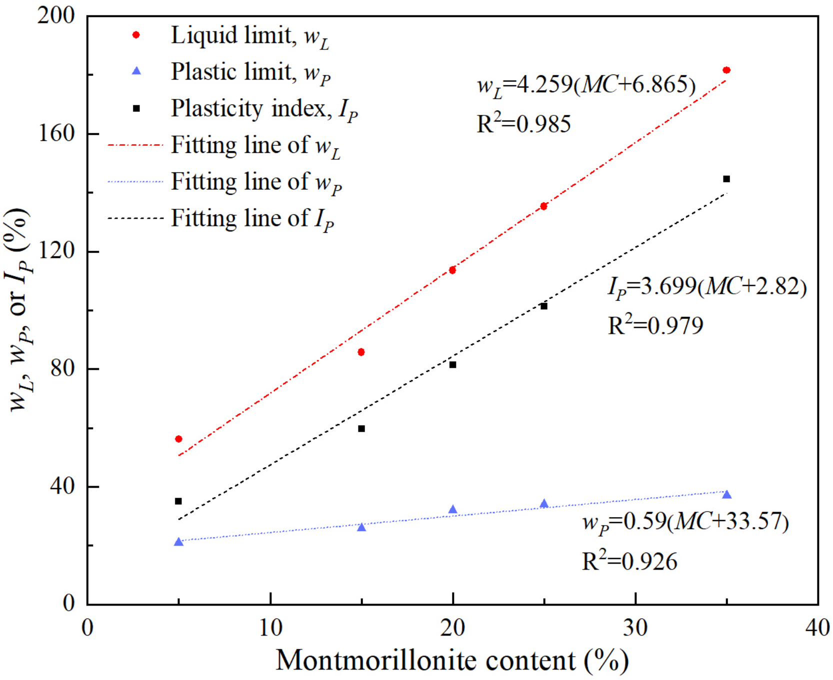

Fig. 2 Relationships of montmorillonite content with liquid and plastic limits as well as plasticity index

In the meantime, plasticity was utilized in this study. A- and U-line are plotted in Fig. 3. It was observed that all the plasticity points of montmorillonite-soil mixtures fall above the A-line and the liquid limit of all specimens are beyond 50%. This indicates that the tested samples are high plastic fine sandy and silty clays. A regression equation between I_P and w_L for montmorillonite-soil mixtures was determined from linear fitting, as shown in Eq. (4).

$$I_p = 0.87(w_L - 17.6) \tag{4}$$

The R^2 value of correlation is 0.997. The following correlations adopted Eq. (4) to describe the relationship between I_P and w_L for montmorillonite-soil mixtures.

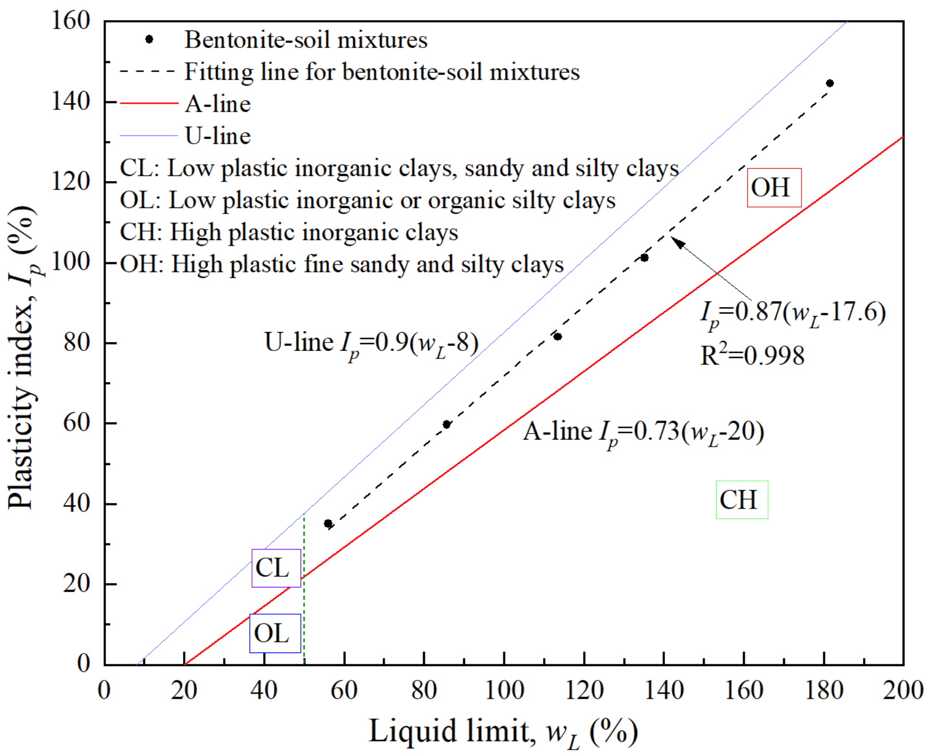

Fig. 3 Plasticity of bentonite-soil mixtures

Correlations of compression index

Skempton (1944) was among the first ones to correlate C_c with liquid limit, whose correlation is widely used. Subsequently, most of the correlations for predicting C_c by use of the Atterberg limit, initial void ratio, and the void ratio at liquid limit have been presented by some researchers. However, these correlations are usually limited to a specific type of soil. Concerning bentonite-soil mixtures, the correlations between C_c and the various indices of five specimens were presented in the following sections.

Liquid limit

Plenty of correlations between C_c and w_L were proposed in the past decades (Skempton, 1944; Terzaghi & Peck, 1948; Nakase et al., 1988; Yin, 1999b; Tiwari & Ajmera, 2012). Among them, a linear correlation between the compression index and liquid limit for HKMD was presented by Yin (1999b). However, a large portion of clay minerals in HKMD are kaolinite and illite (Tovey, 1986) whose properties are greatly different from those of montmorillonite.

The curves of void ratio versus the logarithm of vertical effective stress (e-log(σ_v) curves) are depicted in Fig. 4, from which the compression index was determined for all five specimens. To better estimate the C_c values of bentonite-soil mixtures, the variation of compression index with liquid limit and a best-fitting line for mixtures are plotted in Fig. 5(a). A correlation between C_c and w_L was displayed in Eq. (5), with an R^2 value of 0.994.

$$C_c = 0.0141 w_L - 0.516 \tag{5}$$

Several regression lines from the literature are also presented in Fig. 5(a). It can be observed that experimental data were not in good agreement with these regression lines. Compared with the line proposed by Tiwari and Ajmera (2012) and produced based on the oedometer results of montmorillonite-sand mixtures, Tiwari's line was found to lie above the fitting line obtained from this study. This observation implies that the compression index is not only related to the indexes of soil but also affected by its grain composition. The current correlations for predicting soil parameters are not universal. On this account, it is suggested that future research focus on investigating composition effects on the relationship between soil parameters and index properties.

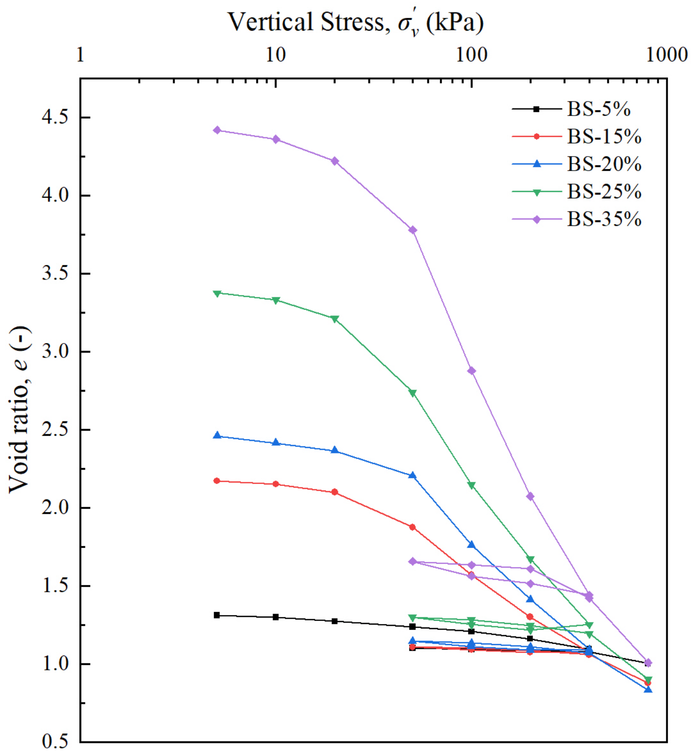

Fig. 4 Variations of void ratio versus the logarithm of vertical stress for five specimens

Plasticity index

The plasticity index is one of the most crucial indices in geotechnical engineering. Nakase et al. (1988) and Tiwari and Ajmera (2012) presented some linear predictive correlations of C_c with plasticity index, as shown in Fig. 5(b). The change of compression index with I_P is also displayed in Fig. 5(b). Thereafter, a new correlation equation expressed in Eq. (6) was obtained with a value of R^2 of 0.996 by linear fitting in the I_p-C_c plane.

$$C_c = 0.0163 I_p - 0.270 \tag{6}$$

It can be noticed that the line proposed by Nakase et al. (1988) is quite diverse from the experimental data of bentonite-soil mixtures. This is because his correlation was produced by the data of marine clay-sand mixtures whose dominated mineral is kaolinite and plasticity index ranged between 10% and 50%.

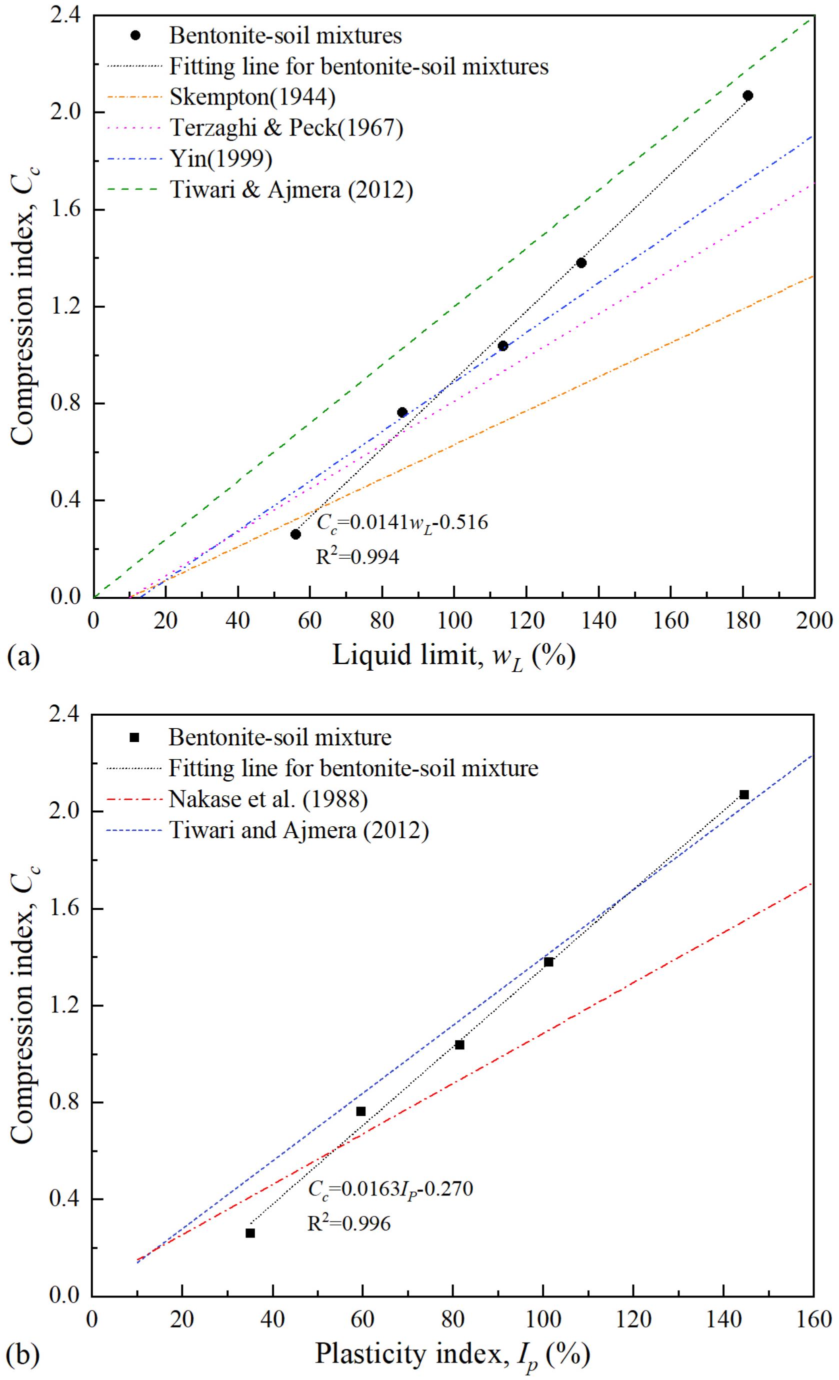

Fig. 5 Variations of compression index with (a) liquid limit and (b) plasticity index

Correlations of swelling index

It appears that the empirical equations for predicting the swelling coefficient are quite limited compared with the number of predictive correlations of compression index presented in the literature. However, some correlations were previously presented in the literature for predicting swelling index, including Nakase et al. (1988), Yin (1999b), and Tiwari and Ajmera (2011). As indicated by Alonso et al. (1999), the swelling behavior of expansive soils is of significance to geotechnical engineering. As known to all, bentonite is a typical highly expansive soil. Thus, the swelling index was determined for five specimens from *e*-log*σ'* curves, as shown in Fig. 4. The results of correlation for predicting the swelling index with liquid limit or plasticity index were illustrated in the following sections.

Liquid limit

The change of swelling index with liquid limit is depicted in Fig. 6(a). A corresponding regression equation with an R^2 value of 0.988 was obtained from the data of bentonite-soil mixtures tested in this study, as expressed in Eq. (7).

$$C_s = 0.0021 w_L - 0.075 \quad (7)$$

Two correlations of the swelling index and liquid limit available in the literature (Yin, 1999b; Tiwari & Ajmera, 2011) are also plotted in Fig. 6(a) for comparison. The correlation between C_s and the liquid limit is well linear, differing from the quadratic correlations deduced by Tiwari and Ajmera (2011) based on the results of different clay dominant soils. It was discovered that the linear correlation proposed by Yin (1999b) could capture the part of the trend of C_s for the tested mixtures with a liquid limit of lower than 80%. Nevertheless, the swelling index estimated using Tiwari's quadratic equation was greatly distinct from the experimental finding with a significantly greater value. Therefore, Eq. (7) was recommended for predicting the swelling index of bentonite-soil mixtures if liquid limit was known.

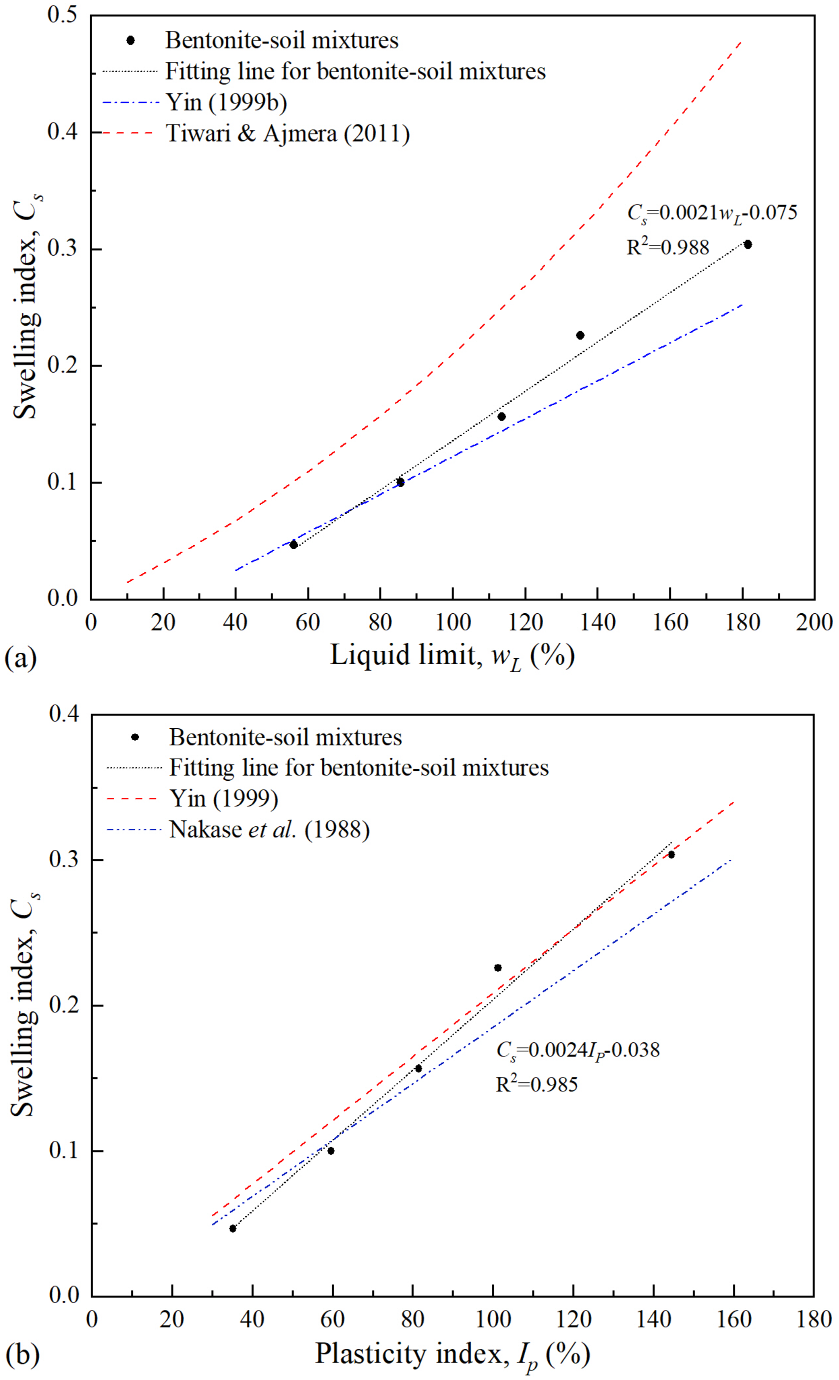

Fig. 6 Changes in swelling index with (a) liquid limit and (b) plasticity index

Plasticity index

Correlations of the swelling index with the plasticity index have been presented by some scholars (Nakase et al., 1988; Yin, 1999b; Kordnaeij et al., 2015). A regression line plotted by using the data of C_s and I_P is shown in Fig. 6(b). With a coefficient of determination of 0.985, the corresponding correlation was expressed in Eq. (8).

$$C_s = 0.0024 I_p - 0.038 \tag{8}$$

Meanwhile, two regression lines from previous research are plotted in Fig. 6(b) as well for comparison with the fitting line generated from the experimental data in the present investigation. It can be noticed that the three lines are close, and Yin's line is quite similar to that proposed in this study.

Correlations of creep parameters

The time-dependent stress-strain behavior during the loading stage, i.e., creep, was tested in this study. Creep coefficient $C_{\alpha e}$ is a most critical parameter in the design of geotechnical projects, visco-plastic elastic constitutive modeling and long-term settlement calculation (Yin & Graham, 1989; Zhu & Yin, 2000; Yin & Feng, 2017; Yin et al., 2022). Correlating $C_{\alpha e}$ with index properties will contribute to its more convenient use.

$C_{\alpha e}$ values were determined from curves in terms of void ratio versus the logarithm of time for each loading stage with a duration of five days for all tested specimens except the one with a montmorillonite content of 5% because of its low viscosity and less significant time-dependent behavior. The average value of $C_{\alpha e}$ for each specimen was calculated and utilized to establish relationships with Atterberg limit indices. Besides, two nonlinear parameters in the nonlinear creep function proposed by Yin (1999a) and used by numerous researchers (Mesri & Vardhanabhuti, 2005; Shen &

Xu, 2011; Le et al., 2017) were also computed for the soil specimens under a constant loading of 100 kPa and correlated with liquid limit and plasticity index.

Liquid limit

A correlation was presented by Zhu et al. (2016) in terms of creep coefficient and the combination of liquid limit and water content, which however was somewhat complicated. The variation of creep coefficient with w_L is shown in Fig. 7. The regression polynomial equation presented in Eq. (9) was obtained from the curve, with an R^2 value of 0.997, indicating a good fit.

$$C_{\alpha e} = 1.67 \times 10^{-5} (w_L)^2 - 5.29 \times 10^{-6} w_L - 0.0017 \quad (9)$$

Apart from that, a correlation between the creep coefficient and plasticity index proposed by Yin (1999b) is also shown in Fig. 7 for comparison. It was found that the equation proposed by Yin (1999b) for HKMD with different clay contents could not predict the $C_{\alpha e}$ value of bentonite-soil mixtures used in this study well. Moreover, the predicted values are much greater than the values measured from oedometer tests. One reason is that kaolinite and illite are the dominated clay minerals of HKMD, while montmorillonite is the main composition of the mixture in this study. Montmorillonite is the most viscous of the three main clay minerals. The different properties of the three clay minerals, especially viscosity property, give rise to significant distinctions in the liquid limit, plasticity index and the $C_{\alpha e}$ values between bentonite-soil mixtures and HKMD. Another reason is that the matrix soil of the mixture used in this study is bentonite, a construction waste which may contain a mass of sand, drilling slag, residue from poured concrete, curing agents, *etc*. The increase of granular materials resulted in the obviously increased permeability of the soil mixture. Furthermore, the viscosity of the clay mixture decreased with the increasing percentage of granular materials.

Plasticity index

A quadratic curve is also plotted in Fig. 7 to fit the creep coefficient with the plasticity index, and the corresponding correlation was given by Eq. (10). It was found that the value of the determination coefficient is 0.998 and the creep coefficient can be captured by the proposed correlation well.

$$C_{\alpha e} = 1.48 \times 10^{-6} (I_p)^2 + 1.41 \times 10^{-4} I_p - 0.0076 \tag{10}$$

It can be observed from Fig. 7 that the trend of the two regression curves plotted by liquid limit and plasticity index are identical.

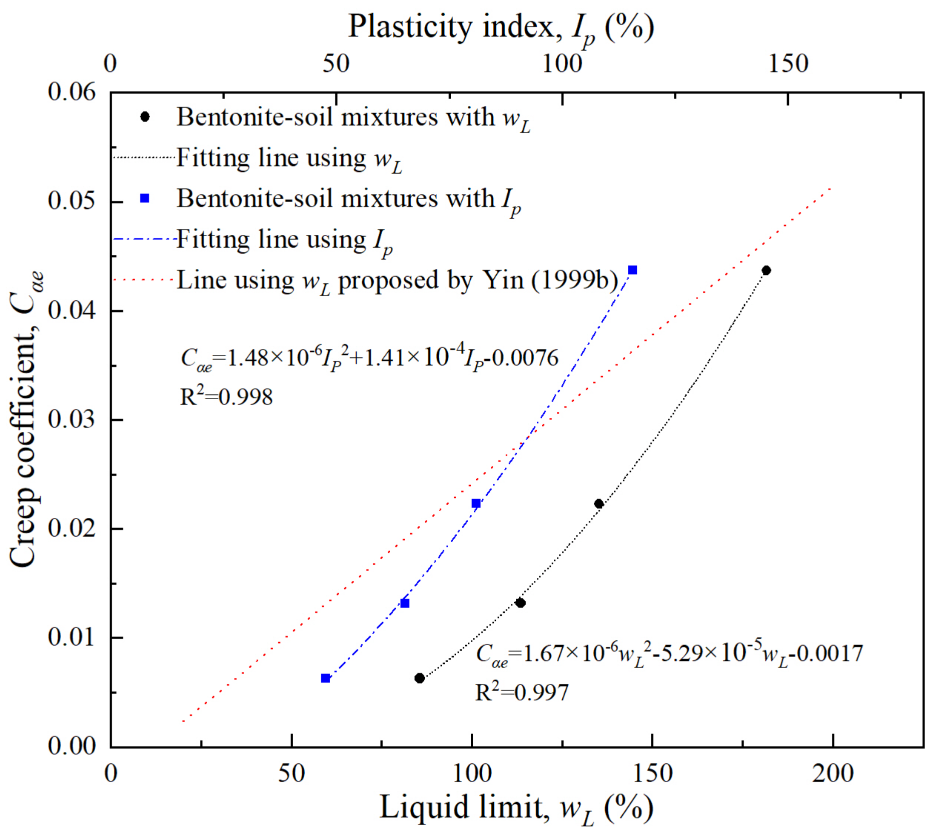

Fig. 7 Variations of creep coefficient with liquid limit or plasticity index

Correlations of parameters in the nonlinear creep function

The great bulk of conventional equations for the analysis of time-dependent behavior were based on the linear correlations between creep strain and the logarithm of time. Nevertheless, one limitation of the linear creep function is that strain will be infinite when time is equal to infiniteness, which is not in line with the scientific foundation. Hence, a non-linear creep function was put forward by Yin (1999a) to incorporate the influence of the decreasing creep parameter with time, which was expressed as follows:

$$\Delta\varepsilon_z = \frac{\psi_0 / V}{1 + \frac{\psi_0}{\varepsilon_c^l V}\ln[(t_0 + t_e)/t_0]}\ln[(t_0 + t_e)/t_0]$$
$$\frac{\ln[(t_0 + t_e)/t_0]}{\Delta\varepsilon_z} = \frac{V}{\psi_0} + \frac{1}{\varepsilon_c^l}\ln[(t_0 + t_e)/t_0] \quad (11)$$

where ψ_0 is a material parameter; ε_c^l is creep strain limit when time is infinite; t_0 is the time parameter to express the beginning of creep behavior; t_e is the equivalent time related to creep. Notably, the time parameter t_0 was considered a constant material parameter.

The values of the nonlinear creep parameter and limit strain for all the specimens with different montmorillonite contents under the stress of 100 kPa were calculated by curve fitting with Eq. (11). Fig. 8 displays the typical fitting curve with the nonlinear creep function plotted by the experimental data of BS-25%. It can be observed that a linear equation of the form $y=ax+b$ was determined with an R^2 value of 0.9986, indicating good curve fitting. According to Eq. (11), the slope of the fitting curve corresponded to $\frac{1}{\varepsilon_c^l}$ and the intercept corresponded to $\frac{V}{\psi_0}$. The values of ε_c^l and ψ_0 were thus obtained.

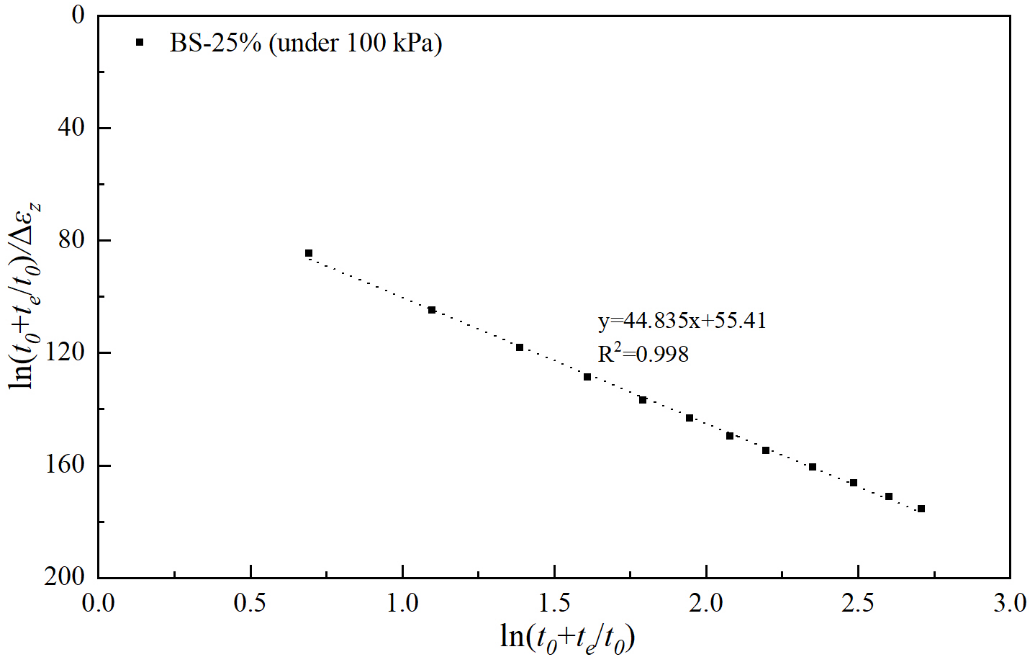

Fig. 8 Typical fitting curve with the nonlinear creep function for BS-25% under 100 kPa

Figs. 9(a) and (b) show the relations between the two parameters of the nonlinear creep function and Atterberg limit indices. Further, corresponding correlations were produced and given in Eqs. (12) to (15).

$$\varepsilon_c^l = 2.59\times10^{-6}(w_L)^2 - 3.46\times10^{-4}w_L + 0.0212 \tag{12}$$

$$\psi_0 = 2.53\times10^{-5}(w_L)^2 - 00432w_L + 0.196 \tag{13}$$

$$\varepsilon_c^l = 2.76\times10^{-6}(I_p)^2 - 1.72\times10^{-4}I_p + 0.011 \tag{14}$$

$$\psi_0 = 2.86\times10^{-5}(I_p)^2 - 0.00307I_p + 0.093 \tag{15}$$

It can be discovered that their determination coefficients are quite close, which are all around 0.99. The predicted values can be employed in both engineering practice and numerical modeling, but the related index properties of soils should be in the tested range. Any extension beyond this range should be checked.

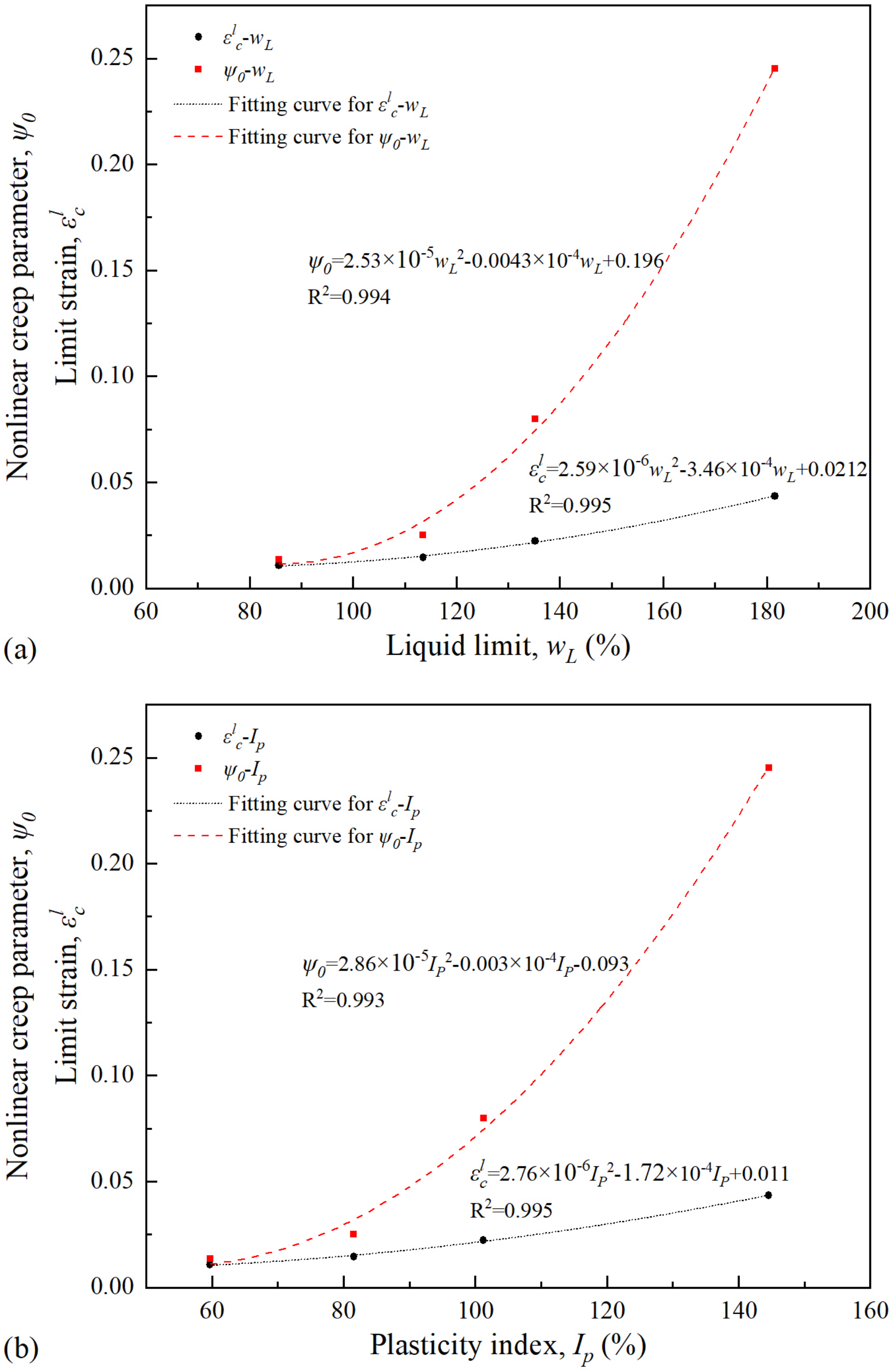

Fig. 9 Relationships between nonlinear parameters and (a) liquid limit and (b) plasticity index

Verification of the proposed correlations using the data from published literature

Based on the oedometer test results of bentonite-soil mixtures, several correlations were proposed to estimate soil parameters, including compression and swelling indices, creep coefficient, nonlinear creep parameter as well as limit strain. Although the correlations were derived from a specific soil type, some of them were also adopted to estimate the parameters of different types of soil, whose data were collected from previous literature. Since liquid limit and plasticity index are more common in geotechnical engineering, verification studies with published data focused on the correlations with w_L and I_p.

Prediction of compression index

Data pertinent to the liquid limit and plasticity index of 30 different soils collected from previous literature (Yin, 1999b; Sridharan & Nagaraj, 2000; Cerato & Lutenegger, 2004; Tong & Yin, 2011; Tiwari & Ajmera, 2012; Feng et al., 2017) were utilized to calculate the compression index with Eqs. (5) and (6). Soil specimens were divided into two groups according to mineral components. The first one is KIDSs, and the other one is MDSs. The scatter plots of the predicted C_c value for soil specimens in previous literature using the newly proposed correlations are presented in Figs. 10(a) and (b). The range interval of ±10% of the measured C_c value was also determined by two plotted lines in the two figures. It can be observed from both figures that the proposed correlations can predict the C_c value with an acceptable accuracy of roughly 90% using the liquid limit and plasticity index for MDSs.

Nevertheless, the predicted results with the correlation using I_p were more accurate than those using w_L. However, it seems that neither I_p nor the w_L correlation can accurately estimate the C_c value for KIDSs. This phenomenon can be attributed to two aspects. On the one hand, the index values of KIDSs are generally smaller than the index range of the soils used in this study. On the other hand, differences in the properties of montmorillonite and kaolin exert a significant impact on the behavior of soils. By and large, it can be considered that the proposed correlations are suitable for estimating the C_c value only for soils with a liquid limit of 40-200% or a plasticity index of 40-160%.

At the same time, the predicted results using the correlations proposed by Skempton (1944) and Yin (1999b), and the corresponding mean absolute error (MAE) values of prediction with different correlations are demonstrated in Figs. 10(a) and (b) for comparison, respectively. It can be seen that the prediction result of Skempton's equation is much smaller than the actual value when the soil has a C_c value greater than 0.5. In other words, Skempton's equation is not suitable for estimating the compression index of MDSs. The accuracy of the prediction results obtained using Yin's equation with I_p is within an acceptable range. For both KIDSs and MDSs, the correlations proposed in this study yielded the lowest MAE values compared with the previous equation in the literature. In addition, the correlation of C_c with I_P outperformed that with w_L as its prediction result has a lower MAE value.

Prediction of swelling index

The liquid limit and plasticity index (Yin, 1999b; Tiwari & Marui, 2005; Tong & Yin, 2011; Kordnaeij et al., 2015) of various soils available in the literature were collected to estimate the swelling index using Eqs. (7) and (8). The relationship between the measured and predicted C_s using liquid limit is plotted in Fig. 11(a), and that using plasticity index is plotted in Figs. 11(b). It can be found that the predicted results of C_s with w_L and I_p could match the measured C_s values well for almost the selected soil specimens from the literature. MAE values can be compared to find that the estimated C_s values using w_L and I_p are quite close, but the correlation with liquid limit exhibited a relatively high level of agreement with the measured C_s values than that using plasticity index. Hence, it was recommended to adopt Eq. (7) to estimate the swelling index of soils.

Prediction of creep coefficient

Detailed information regarding liquid limit, plasticity index, creep coefficient and nonlinear creep behavior was gathered from literature, including Yin (1999a), Yin (1999b), Tong and Yin (2011), Zeng et al. (2012), Zhu et al. (2016), and Feng et al. (2017). These data were applied to estimate creep coefficient and nonlinear creep behavior with equations using liquid limit or plasticity index. The estimated results of $C_{\alpha e}$ are plotted against the measured ones in Figs. 12(a) and (b). It can be seen that using liquid limit to predict creep coefficient yielded a lower MAE value than using plasticity index. Correlations with w_L and I_p could provide an accuracy of 90% for some types of soil, which however could estimate the $C_{\alpha e}$ value with an accuracy of only 50% for other types of soil. The possible reason why the correlation cannot predict the $C_{\alpha e}$ value well is that creep behavior is complicated and associated with a few factors such as micro-pores, particle sliding and internal structure arrangement. As a result, it was suggested that the newly proposed correlations only estimate the creep coefficient of bentonite-soil mixtures or soils with a similar composition of the mixtures used in this study.

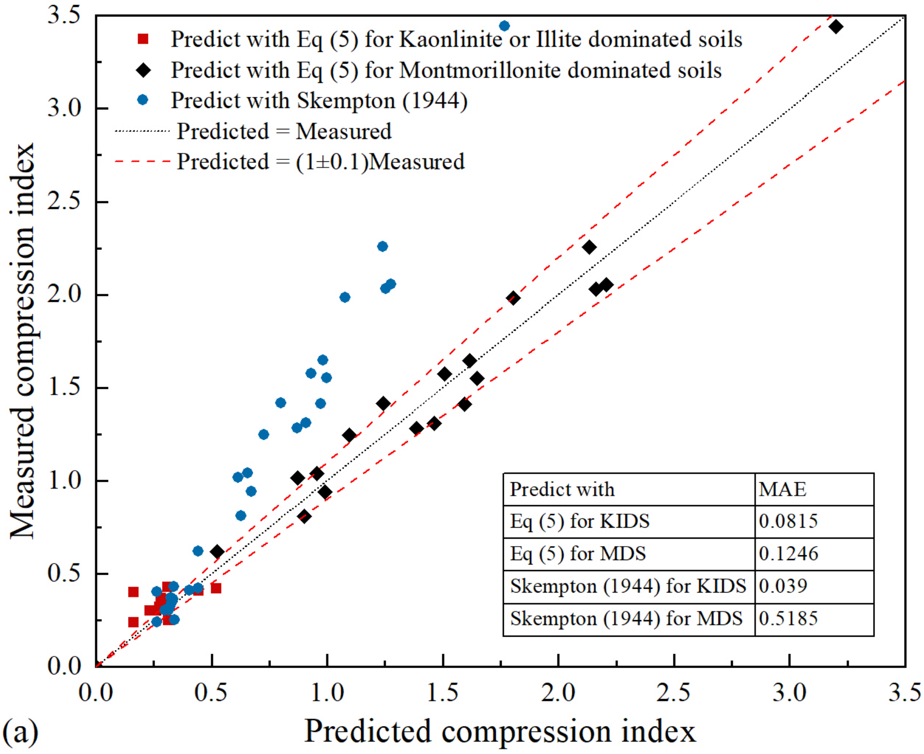

(a)

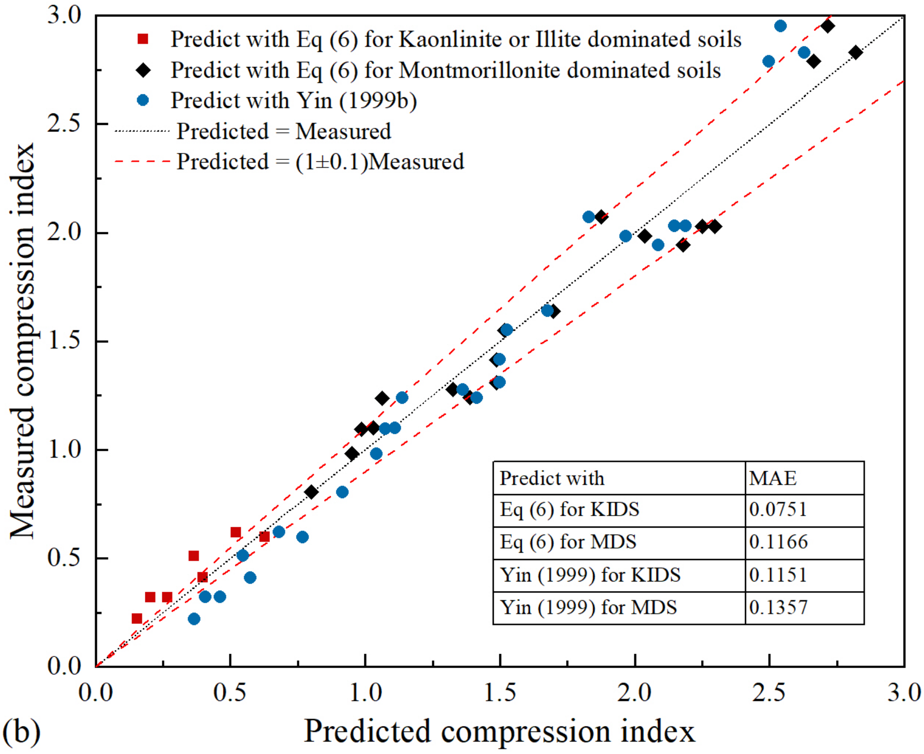

(b)

Fig. 10 Measured C_c against the predicted C_c using (a) Eq (5) and (b) Eq (6) with the published data

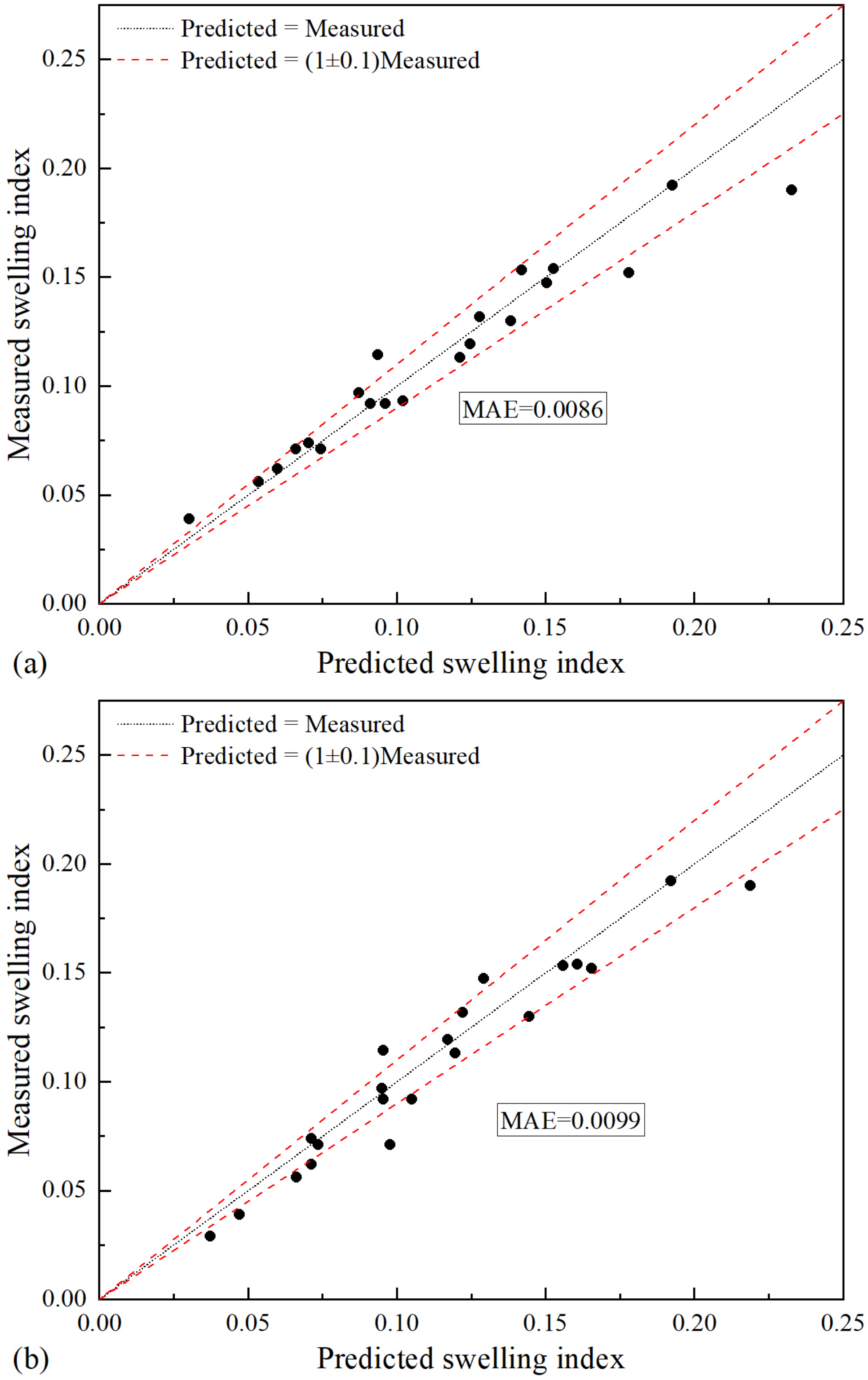

Fig. 11 Measured C_s against the predicted C_s using (a) liquid limit and (b) plasticity index with the published data

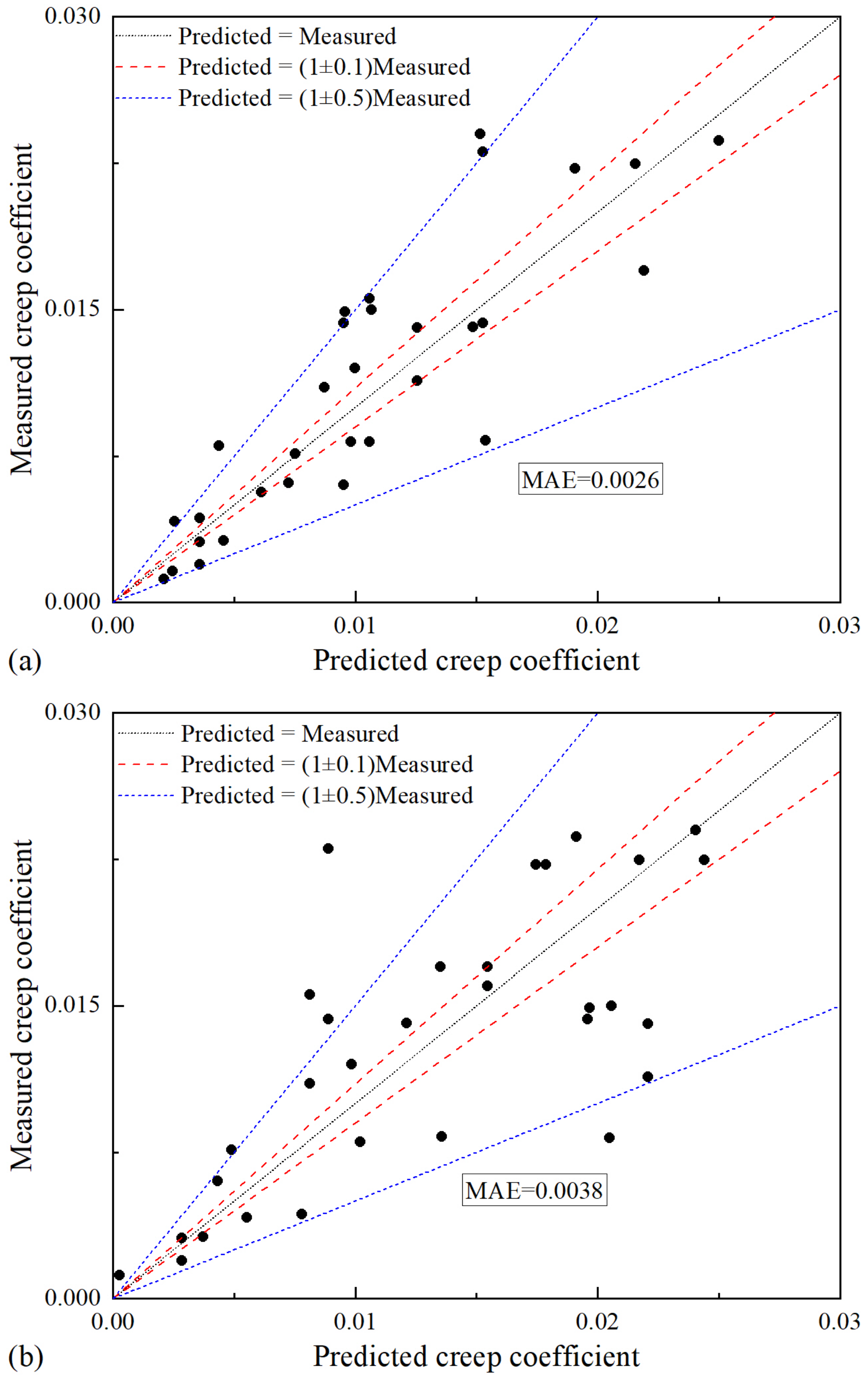

Fig. 12 Measured $C_{\alpha e}$ versus the predicted $C_{\alpha e}$ using (a) liquid limit and (b) plasticity index with the published data

The simplified model with a homogenization approach for hydraulic conductivity

Hydraulic conductivity is an all-important property of clayey soils. Previous works on the hydraulic conductivity of sand-clay mixtures have been investigated, and some different methods of predicting hydraulic conductivity have been brought up (Pandian et al., 1995; Sivapullaiah et al., 2000; Ozhan, 2021). Most of these methods empirically correlated hydraulic conductivity with a liquid limit or corresponding void ratios. Shi and Yin (2018) summarized the influence of sand fraction on the hydraulic conductivity of sand-clay mixtures from previous literature. Additionally, a theoretical model with a homogenization approach was presented to estimate the hydraulic conductivity of sand-marine clay mixtures. Shi and Zhao (2020) held that mixtures with high fine fractions can be simplified as binary mixtures. Thus, bentonite-soil mixtures used in this study and containing bentonite matrix and incompressible sand inclusions can be regarded as binary mixtures. On this account, the model with a homogenization approach proposed by Shi and Yin (2018) can be used for predicting the evolution of hydraulic conductivity for bentonite-soil mixtures in oedometer conditions. This model can be simplified to only three model parameters to make it easier for practical use.

State-dependent variables

Local and overall state-dependent variables were defined and obtained from a series of oedometer tests based on the assumption that sand inclusions are incompressible and impermeable because of being stiffer than the clay matrix and unable to hold water. The absorbed water was associated with the bentonite matrix. The bentonite-soil mixture is composed of three phases: sand inclusion, fluid and bentonite clay matrix phases. Based on the assumption made above, the volume fraction of the sand inclusion ϕ_s can be expressed as

$$\phi_s = \frac{V_s}{V_s + V_b + V_f} = \frac{e_b - e}{(1+e)e_b} \tag{16}$$

where V_s, V_b and V_f denote the volume of sand inclusion, bentonite clay matrix and fluid phases, respectively; $e = V_f/(V_b + V_s)$, representing the overall void ratio of the mixture; $e_b = V_f/V_b$, referring to the local void ratio of the bentonite matrix.

Considering the incompressibility of the sand phase and the association between all moisture and the bentonite matrix, the local void ratio can be expressed as follows:

$$e_b = \frac{(1-\upsilon)\rho_s + \upsilon\rho_b}{(1-\upsilon)\rho_s} e \tag{17}$$

where υ represents the dry mass fraction of sand inclusion in the binary mixture; ρ_s, and ρ_b are the particle density of the sand inclusion and pure bentonite, respectively.

The overall void ratio e was given as a function of overall strain as follows:

$$e = V \exp(-\varepsilon) - 1 \tag{18}$$

where V is the overall specific volume and $\varepsilon = \ln(h_0/h)$ is logarithmic strain.

Previous research has shown that a nonuniform stress distribution exists in the binary mixture owing to the significantly different stiffnesses of constituents (Jamei et al., 2013; Zhuang et al., 2017; Shi et al., 2020). Therefore, σ' and σ_b' were utilized to express the overall effective stress of the bentonite-soil mixture and the local effective stress of bentonite clay.

Simplified homogenization approach

The values of hydraulic conductivity k of all bentonite-soil mixtures were determined for a variety of incremental overall effective stresses (50-800 kPa) from the results of oedometer tests following BS1377 (2016). The evolution of the overall hydraulic conductivity with the increase of the overall effective stress on a double logarithmic scale is illustrated in Fig. 13(a). One can observe that the overall hydraulic conductivity decreased with the increase of both vertical stress and bentonite content. This is because that bentonite has strong hydrophility in the matrix, thus resulting in a decrease in permeability (Pandian et al., 1995). According to the equations given above, state-dependent variables were calculated, and the correlation between the local void ratio and overall hydraulic conductivity on a double-logarithmic scale is demonstrated in Fig. 13(b). It is noteworthy that the relationship is nearly linear in the double-logarithmic space, which well agrees with the findings (Zeng et al., 2012; Shi & Yin, 2018) A linear equation was obtained from curve fitting and can be expressed in the following form:

$$\ln(k_b) = K_R + \xi \ln e_b \tag{19}$$

where k_b is the hydraulic conductivity of the pure bentonite; ξ is the slope of the linear line; K_R is a corresponding model parameter when e_b is equal to 1.

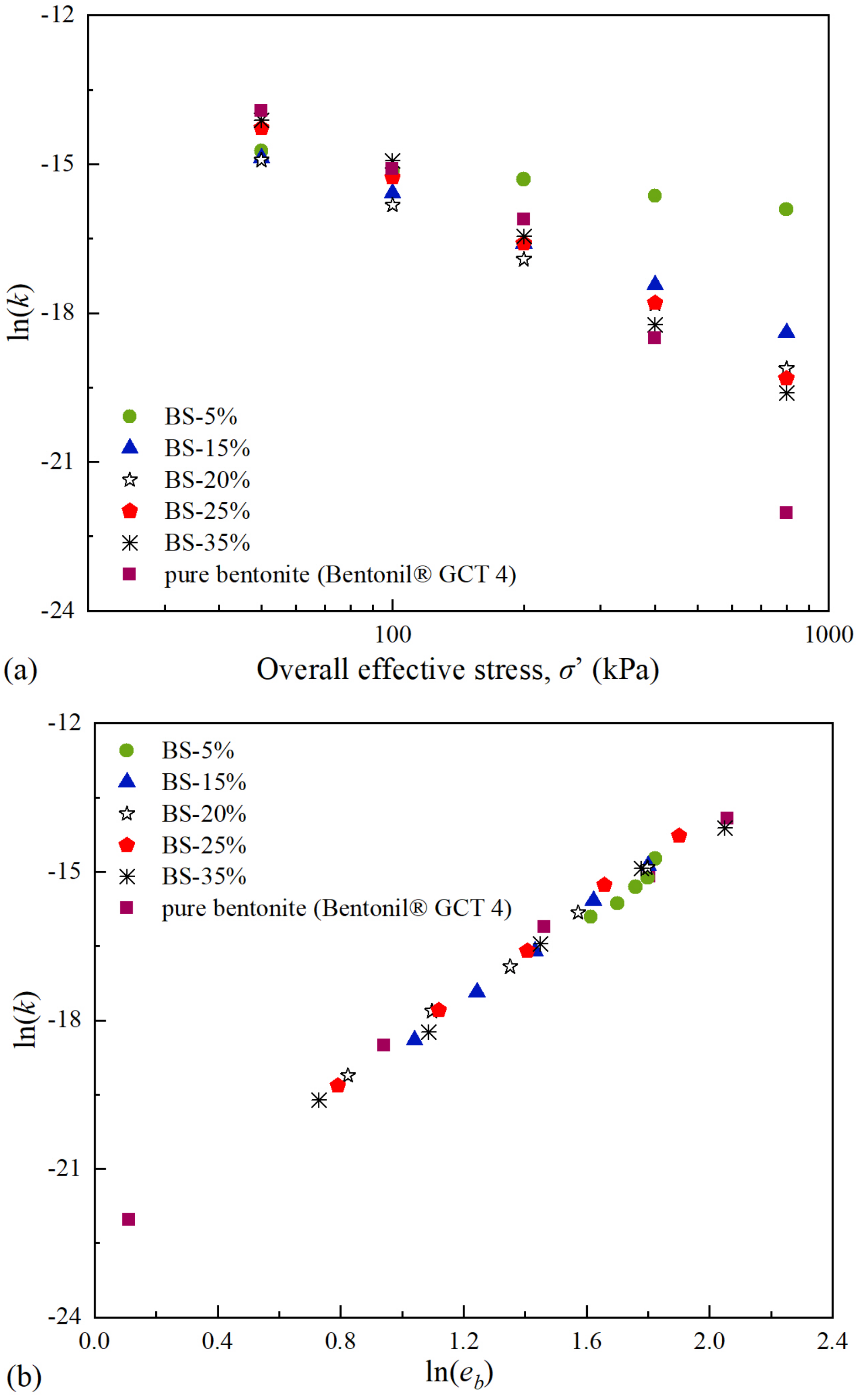

Fig. 13 Evolution of hydraulic conductivity with (a) the overall effective stress and (b) the local void ratio of the bentonite matrix

Eq. (17) can be substituted into Eq. (19) to express the local hydraulic conductivity as a function of the overall void ratio:

$$\ln(k_b) = K_R + \xi \ln[\frac{(1-\upsilon)\rho_s + \upsilon\rho_b}{(1-\upsilon)\rho_s}] + \xi \ln e \tag{20}$$

The model with a homogenization approach proposed by Shi and Yin (2018) was adopted to estimate the evolution of the hydraulic conductivity of bentonite-soil mixtures. In the model, the sand inclusion phase was assumed to be incompressible, and parallel structure and series configurations affected the overall behavior of the binary mixture equivalently. Following the model steps, the overall hydraulic conductivity k was given as a function of k_b as follows:

$$\ln(k) = \eta(1-\phi_s)\ln(k_b) \tag{21}$$

where η is a structure variable, representing the intergranular structure evolution of sand inclusions. The structure variable was expressed as:

$$\eta = (\frac{\alpha}{\alpha - \phi_s})^{\beta} \tag{22}$$

where α represents the upper bound of the volume fraction of sand particles and β stands for a constant model parameter controlling the sensitivity of the variable. Details can be referred to Shi and Yin (2018).

The model with a homogenization approach for estimating the overall hydraulic conductivity was set up. Four parameters were included in this model, and the model parameters of the bentonite-soil mixture are listed in Table 4. The comparison between the experimental and predicted results using Eq (21) is displayed in Fig. 14. It can be seen that the reproduced hydraulic conductivity of the bentonite-soil mixture using the model matched with experimental data well.

Table 4 Model parameters for estimating hydraulic conductivity

Clay matrix	K_R	ξ	α	β	Reference
Bentonite	-22.53	4.25	0.71	0.73	This study
HKMC	-18.25	4.35	0.74	0.79	Shi and Yin (2018)
Bentonite	-26.62	6.73	0.77	0.73	Pandian et al. (1995)
Nagoya clay	-18.39	3.65	0.50	0.33	Watabe et al. (2011)
70% Bentonite+ 30% Kaolinite	-25.31	4.17	0.70	0.68	Deng et al. (2017)
Bentonite	-24.17	3.57	0.80	0.62	Sivapullaiah et al. (2000)

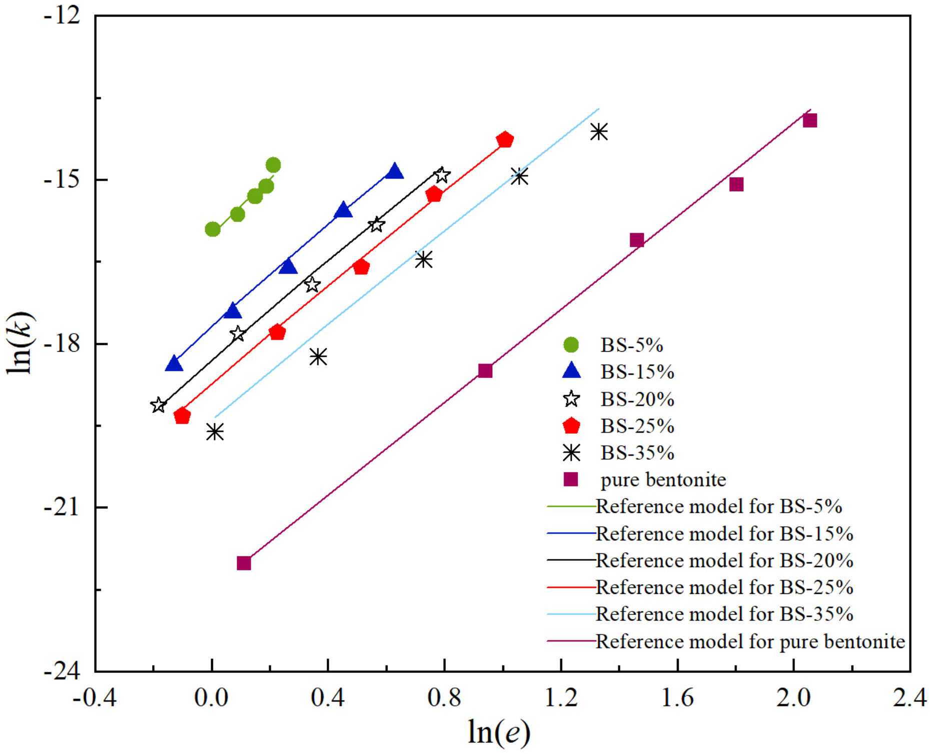

Fig. 14 Comparison between the experimental and predicted results

In the modeling process, however, it was found that the value of $\eta(1-\phi_s)$ ranged from 0.99 to 1.01. The change of values of $\eta(1-\phi_s)$ with ϕ_s for five types of clay-sand mixtures from previous literature (Pandian et al., 1995; Sivapullaiah et al., 2000; Watabe et al., 2011; Deng et al., 2017; Shi & Yin, 2018) was investigated to simplify this homogenization model. The variations of the volume fraction of sand inclusions with the void ratio for the mixture with different sand contents are shown in Fig. 15(a). To consider the limit state, the value of ϕ_s was selected in the range of 0.01 to 0.5. The model parameters α and β of clay-sand mixtures in the literature were kept consistent with Shi and Yin (2018), which are listed in Table 4. The change of the calculated value of $\eta(1-\phi_s)$ with the volume of the sand fraction is presented in Fig. 15(b). It can be observed that the value of $\eta(1-\phi_s)$ ranged from 0.95 to 1.10 and most of the points were located in the range of 0.98 to 1.025.

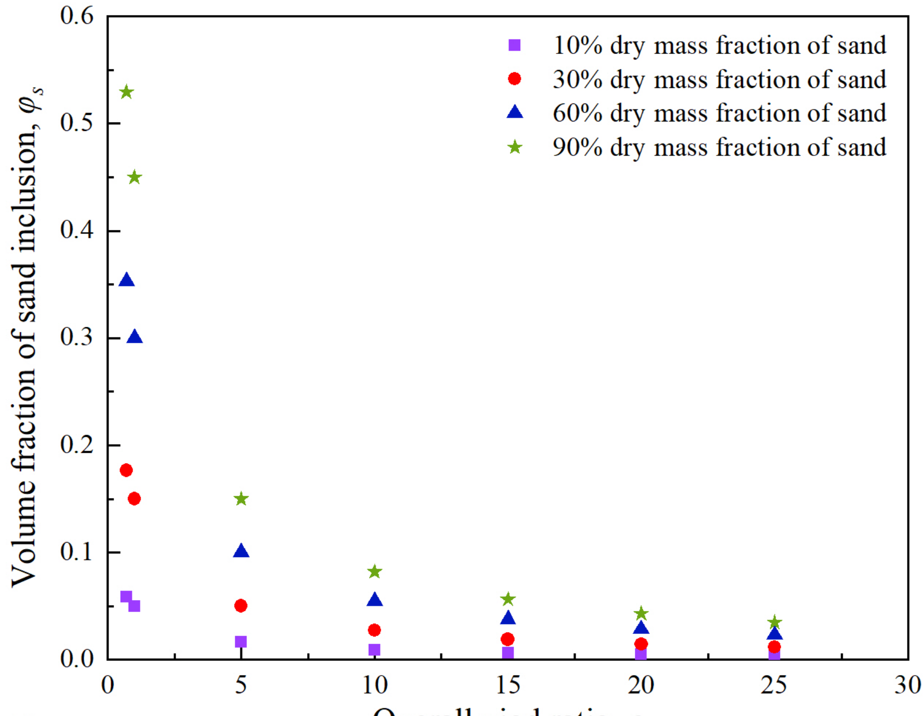

(a)

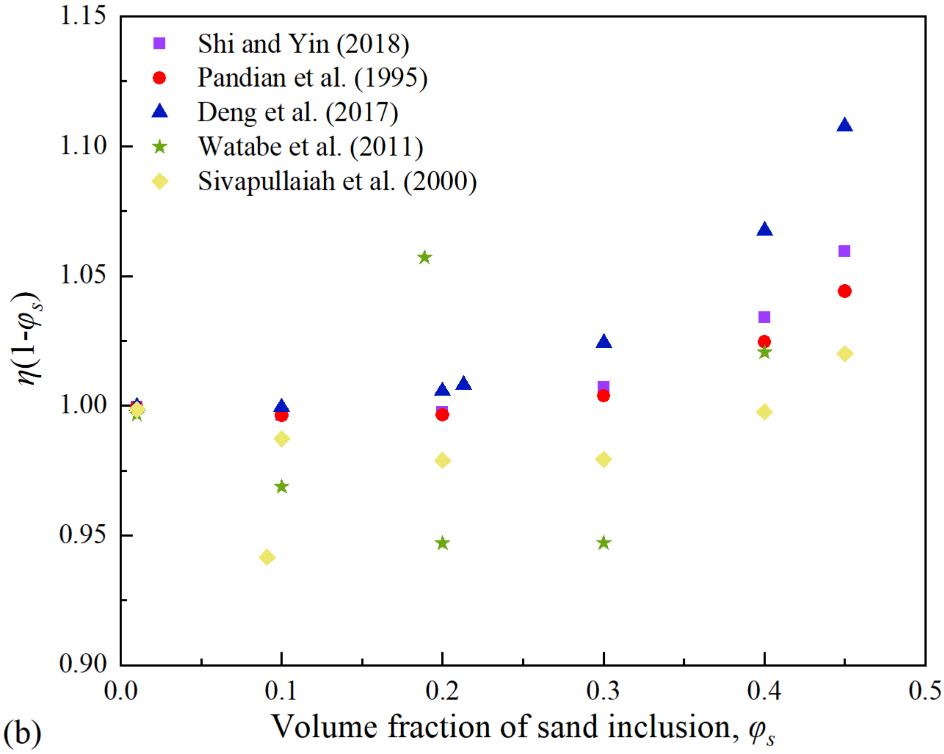

(b)

Fig. 15 (a) Variation of volume fraction of sand with the overall void ratio; (b) change in the $\eta(1-\phi_s)$ value with the volume fraction of sand inclusions for soils

Consequently, the product of the structure variable η and the $(1-\phi_s)$ value had little effect on the overall hydraulic conductivity of most clay-sand mixtures. The theoretical model with a homogenization framework can be simplified to a new form expressed as follows:

$$\ln(k) = \gamma\left[K_R + \xi \ln[\frac{(1-\upsilon)\rho_s + \upsilon\rho_b}{(1-\upsilon)\rho_s}] + \xi \ln e\right] \quad (23)$$

where γ is a model parameter to correlate the local and overall hydraulic conductivity.

For most clay-sand mixtures, the value of γ was recommended to take 1. The model can be further simplified into the form of Eq. (24).

$$\ln(k) = K_R + \xi \ln[\frac{(1-\upsilon)\rho_s + \upsilon\rho_b}{(1-\upsilon)\rho_s}] + \xi \ln e \quad (24)$$

The simplified model was adopted to estimate hydraulic conductivity, and the results were compared with reference ones, as demonstrated in Fig. 16. It can be seen that the calculated results between reference and simplified models are quite close. The simplified homogenization model only has three parameters very easy to be determined from the oedometer tests on pure clay, which thus may be more easily accepted by practical engineering applications. It is worth noting that the $\eta(1-\phi_s)$ value is around 1.1 when the dry mass fraction of sand inclusion is above 90% and the overall void ratio is below 0.5 (see Fig. 15(a)). Hence, the simplified model should be used with caution, and the value of γ can be taken within the range of 1.05 to 1.1 in this extreme case.

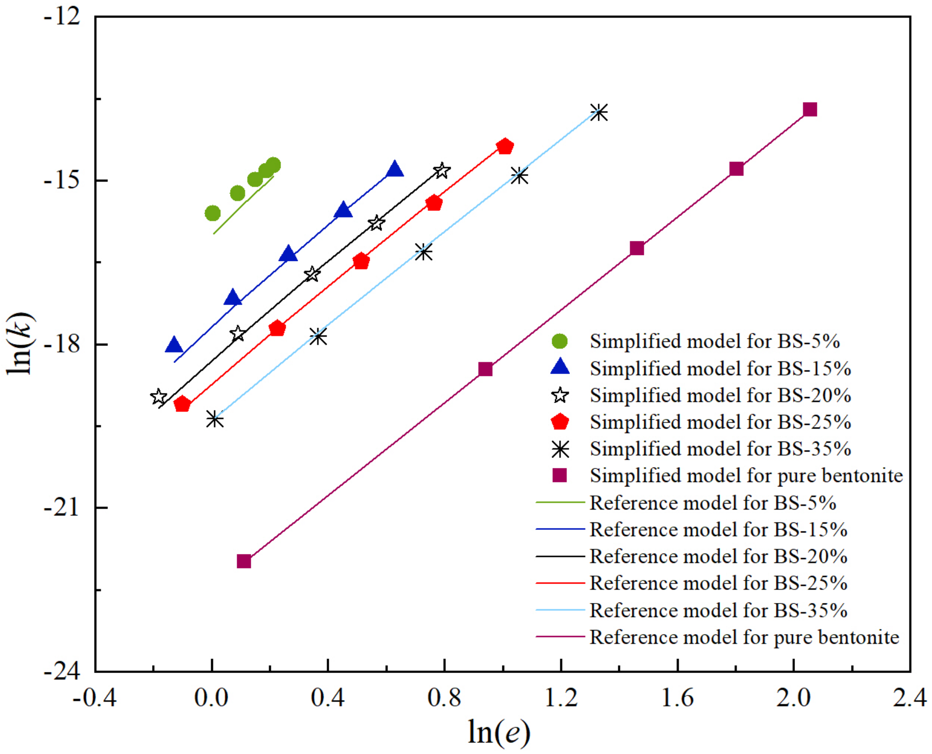

Fig. 16 Comparison between simulation results with simplified and reference models

Microstructure analysis

After oedometer tests, bentonite-soil mixtures were dried by vacuum and cut into cubes for SEM observation. SEM photos with 1,000 × magnification for five specimens are obtained and presented in Figs. 17(a) ~ (e), respectively. Fig. 17(a) shows that silt particles are dominant in the microfabric, and sand particles are independent of each other to form a skeletal structure. However, the number of independent sand particles decreased on account of their closer contact with the bentonite matrix. The honeycomb microstructure of the continuous bentonite clay matrix was gradually developed with the increase of bentonite content (Fig. 17e). The comparison of SEM photos revealed that the diameter of visible pores decreased with the increase of bentonite content. The finding indicates that the large inter pores between sand grains were probably filled up by the bentonite clay matrix and converted to small-sized pores between clay matrix or aggregation and sand particles.

This variation of the microstructure of specimens reflected the increasing compressibility with the increase of montmorillonite content. The diameter of pores ranged from 1 to 5 μm in the BS-35% specimen and 5 to 20 μm in the BS-5% one. This result is consistent with the findings of Watabe et al. (2011) and the compressibility behavior in this study.

The more visible microfabric of BS-5% and -35% specimens magnified at 5,000 times are displayed in Figs. 18(a) and (b). The bonds between clay are dominated by the formation of edge-to-face and -edge in the microfabric of BS-35% (Fig. 18b), whereas the interaction of BS-5% specimens mainly features face-to-face formation. As presented in Fig. 18(a), it appears that the clay particle or matrix tended to form aggregation or accumulate at the contact points of adjacent sand particles or on the surface of independent sand particles. The densification of the clay contributed to the formation of clay bridges. Similarly, Gratchev et al. (2007) found a similar bridge-like structure in a bentonite-sand mixture, but the clay bridge seemed to disappear and the microfabric became more homogeneous in the BS-35% specimen compared with that in Fig. 18(a). With the homogenization approach, the clay bridge can clarify the different mechanisms of binary sand-clay mixtures, where stress distribution is non-uniform since the clay bridge could bear more stress. With the increase in sand fraction, the number of clay bridges increased, hence increasing the heterogeneity of binary mixtures (Fei, 2016; Shi et al., 2018). In short, the clay bridge is important in the homogenization approach since it may significantly affect the strain and stress distribution in soils.

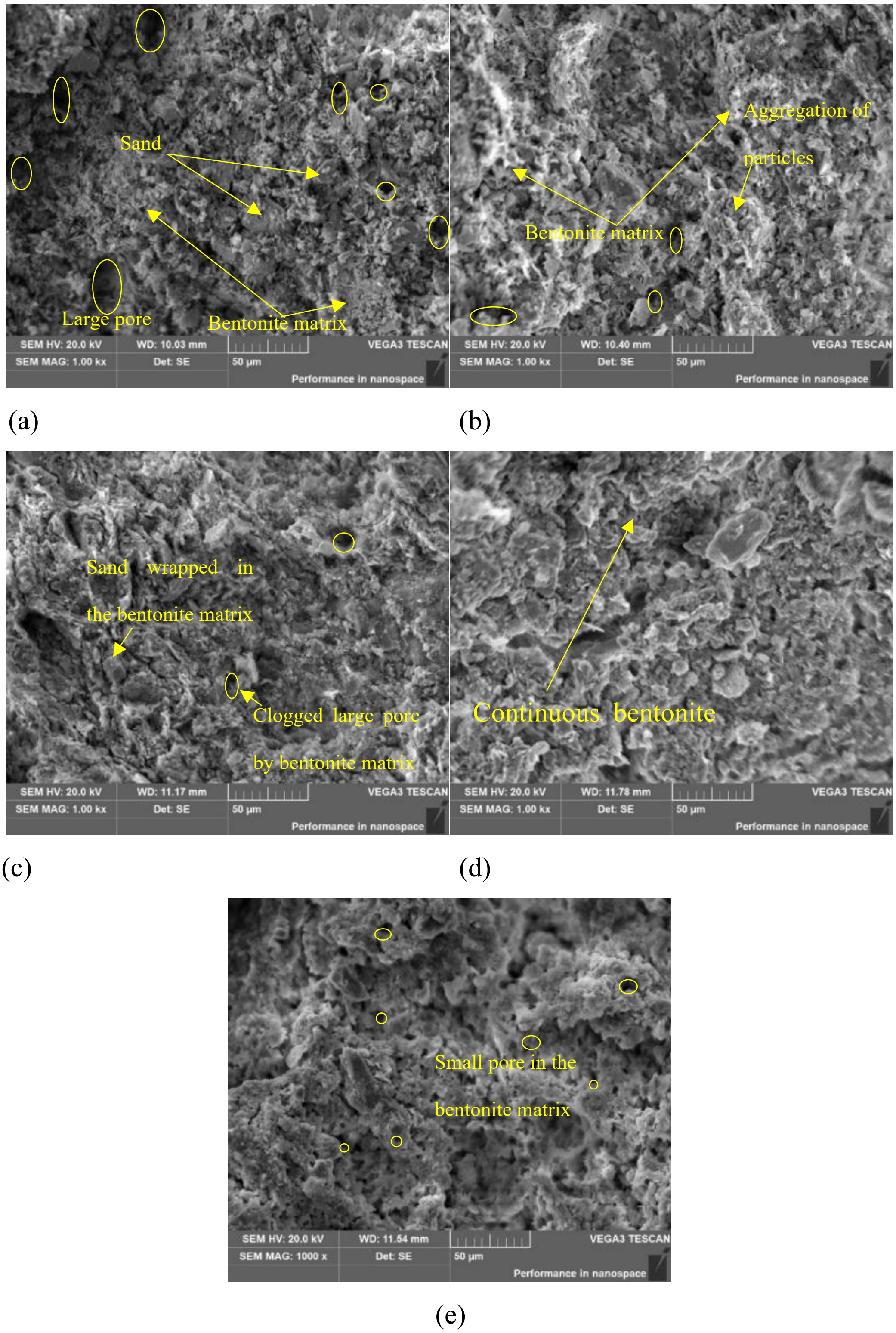

Fig. 17 SEM photos with 1,000 × magnification for bentonite-soil mixtures: (a) BS-5%, (b) BS-15%, (c) BS-20%, (d) BS-25% and (e) BS-35%

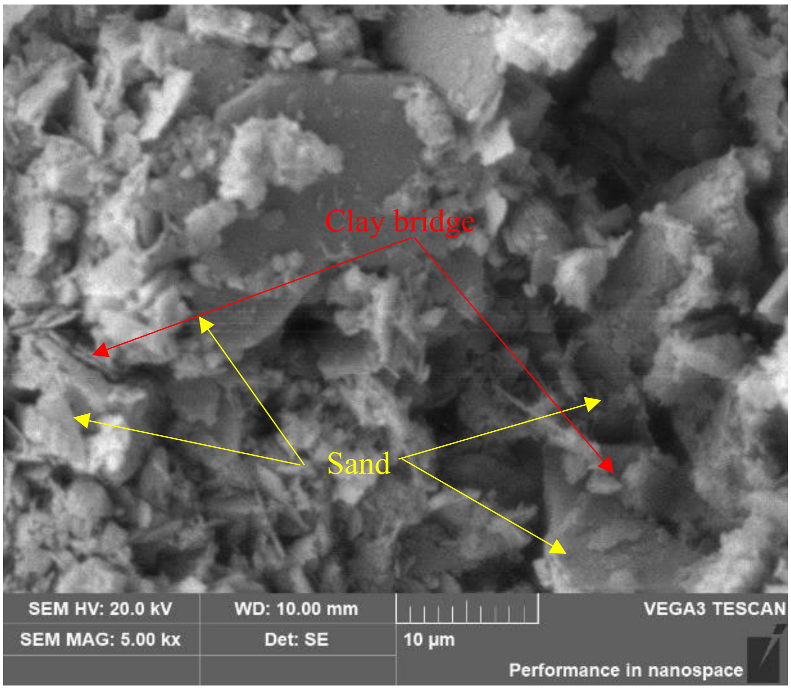

(a)

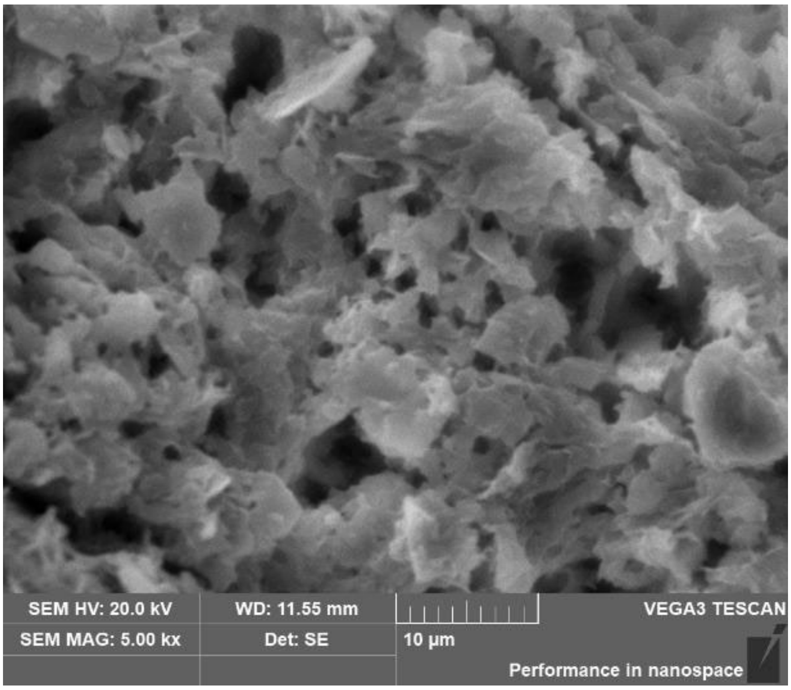

(b)

Fig. 18 SEM photos of (a) BS-5% and (b) BS-35% with 5,000× magnification

Conclusions

In this paper, the results of mineralogic composition, index properties and the consolidation behavior from the oedometer tests of reconstituted bentonite-soil mixture specimens with different montmorillonite contents were presented, analyzed and discussed. Several correlations were proposed to estimate the values of C_c, C_s, $C_{\alpha e}$, ε_c^l and ψ_0 with easily accessible index properties. A simplified model with a homogenization approach was put forward to predict the hydraulic conductivity at different vertical stresses. Some of the newly proposed correlations were verified by the use of the data collected from previous literature. The main conclusions drawn from this comprehensive experimental study are as follows:

(1) Mechanical parameters, including C_c, C_s and $C_{\alpha e}$, are closely related to the montmorillonite content and Atterberg limit indices of the tested specimens. These proposed correlations are capable of estimating the values of mechanical parameters for the majority of montmorillonite-dominated soils in literature with reasonable accuracy.

(2) Parameters in the nonlinear creep function, including ε_c^l, and ψ_0, experienced a significant increase with montmorillonite content. The two nonlinear parameters are also correlated with w_L and I_p with R^2 values larger than 0.9.

(3) A simplified model with a homogenization approach, which only has three model parameters, was developed for easier use. Hydraulic conductivity can be well estimated using the newly proposed model.

(4) A bridge-like structure which was called a clay bridge seemed to exist in bentonite-soil mixtures to bond sand particles. The number of clay bridges increased with the decrease of bentonite content.

(5) The newly proposed correlations were only recommended to estimate parameters of MDSs with Atterberg limit indices in the tested range. Any extension beyond this range must be checked and verified.

Acknowledgments The work in this paper was supported by a Research Impact Fund (RIF) (R5037-18), a Theme-based Research Scheme Fund (TRS) (T22-502/18-R) and three General Research Fund (GRF) projects (The Hong Kong Polytechnic University (PolyU) 152179/18E; PolyU 152130/19E; PolyU 152100/20E) from the Research Grants Council (RGC) of Hong Kong Special Administrative Region Government of China. The authors also acknowledged the financial support of a grant (CD82, CD7A) from Research Institute for Land and Space and grants (ZDBS, BD8U) from PolyU.

Declarations

Conflict of interest The authors declared no competing interests.

References

1377, B S (2016). British Standard 1377, Methods of Test for Soils for Civil Engineering Purposes. In.

Alonso, E, Vaunat, J, & Gens, A (1999) Modelling the mechanical behaviour of expansive clays. Eng Geol 54(1-2), 173-183.

Amarasinghe, P M, Katti, K S, & Katti, D R (2012) Insight into role of clay-fluid molecular interactions on permeability and consolidation behavior of Na-montmorillonite swelling clay. J. Geotech. Geoenviron. Eng. 138(2), 138-146.

Burland, J (1990) On the compressibility and shear strength of natural clays. Géotechnique 40(3), 329-378.

Cerato, A B, & Lutenegger, A J (2004) Determining intrinsic compressibility of fine-grained soils. J. Geotech. Geoenviron. Eng. 130(8), 872-877.

Chapuis, R P (2012) Predicting the saturated hydraulic conductivity of soils: a review. Bull. Eng. Geol. Environ. 71(3), 401-434.

Cozzolino, V. (1961). Statistical forecasting of compression index. In *Proceedings of the 5th international conference on soil mechanics and foundation engineering Paris*.

Deng, Y, Wu, Z, Cui, Y, Liu, S, & Wang, Q (2017) Sand fraction effect on hydro-mechanical behavior of sand-clay mixture. Appl Clay Sci 135, 355-361.

Fei, K (2016) Experimental study of the mechanical behavior of clay–aggregate mixtures. Eng Geol 210, 1-9.

Feng, W-Q, Lalit, B, Yin, Z-Y, & Yin, J-H (2017) Long-term non-linear creep and swelling behavior of Hong Kong marine deposits in oedometer condition. Comput Geotech 84, 1-15.

Gratchev, I B, Sassa, K, Osipov, V I, Fukuoka, H, & Wang, G (2007) Undrained cyclic behavior of bentonite–sand mixtures and factors affecting it. Geotech. Geol. Eng. 25(3), 349-367.

Jamei, M, Villard, P, & Guiras, H (2013) Shear failure criterion based on experimental and modeling results for fiber-reinforced clay. Int. J. Geomech. 13(6), 882-893.

Kordnaeij, A, Kalantary, F, Kordtabar, B, & Mola-Abasi, H (2015) Prediction of recompression index using GMDH-type neural network based on geotechnical soil properties. Soils Found. 55(6), 1335-1345.

Kurnaz, T F, Dagdeviren, U, Yildiz, M, & Ozkan, O (2016) Prediction of compressibility parameters of the soils using artificial neural network. Springerplus 5(1), 1-11.

Le, T M, Fatahi, B, Khabbaz, H, & Sun, W (2017) Numerical optimization applying trust-region reflective least squares algorithm with constraints to optimize the non-linear creep parameters of soft soil. Appl. Math. Model. 41, 236-256.

Mesri, G, & Vardhanabhuti, B (2005) Secondary compression. J. Geotech. Geoenviron. Eng. 131(3), 398-401.

Nagaraj, T, & Murthy, B S (1983) Rationalization of Skempton's compressibility equation. Geotechnique 33(4), 433-443.

Nakase, A, Kamei, T, & Kusakabe, O (1988) Constitutive parameters estimated by plasticity index. Journal of Geotechnical Engineering 114(7), 844-858.

Oscarson, D, Dixon, D, & Gray, M (1990) Swelling capacity and permeability of an unprocessed and a processed bentonitic clay. Eng Geol 28(3-4), 281-289.

Ozhan, H O (2021) Determination of mechanical and hydraulic properties of polyacrylamide-added bentonite-sand mixtures. Bull. Eng. Geol. Environ. 80(3), 2557-2571.

Pandian, N, Nagaraj, T, & Raju, P N (1995) Permeability and compressibility behavior of bentonite-sand/soil mixes. Geotech. Test. J. 18(1), 86-93.

Shen, S-L, & Xu, Y-S (2011) Numerical evaluation of land subsidence induced by groundwater pumping in Shanghai. Can. Geotech. J. 48(9), 1378-1392.

Shi, X, Nie, J, Zhao, J, & Gao, Y (2020) A homogenization equation for the small strain stiffness of gap-graded granular materials. Comput Geotech 121, 103440.

Shi, X, & Yin, J (2018) Estimation of hydraulic conductivity of saturated sand–marine clay mixtures with a homogenization approach. Int. J. Geomech. 18(7), 04018082.

Shi, X, Yin, J, Feng, W, & Chen, W (2018) Creep coefficient of binary sand–bentonite mixtures in oedometer testing using mixture theory. Int. J. Geomech. 18(12), 04018159.

Shi, X, & Zhao, J (2020) Practical estimation of compression behavior of clayey/silty sands using equivalent void-ratio concept. J. Geotech. Geoenviron. Eng. 146(6), 04020046.

Sivapullaiah, P, Sridharan, A, & Stalin, V (2000) Hydraulic conductivity of bentonite-sand mixtures. Can. Geotech. J. 37(2), 406-413.

Skempton, A W (1944) Notes on the compressibility of clays. Quarterly Journal of the Geological Society 100(1-4), 119-135.

Sridharan, A (1999) Volume change behaviour of expansive soils. Problematic soils, 883-850.

Sridharan, A, & Nagaraj, H (2000) Compressibility behaviour of remoulded, fine-grained soils and correlation with index properties. Can. Geotech. J. 37(3), 712-722.

Terzaghi, K, & Peck, R (1948) Soil Mechanics in Engineering Practice (Fourth Printing). John Wilfy & Sons Inc., New York, NY, USA.

Tiwari, B, & Ajmera, B (2011) Consolidation and swelling behavior of major clay minerals and their mixtures. Appl Clay Sci 54(3-4), 264-273.

Tiwari, B, & Ajmera, B (2012) New correlation equations for compression index of remolded clays. J. Geotech. Geoenviron. Eng. 138(6), 757-762.

Tiwari, B, & Marui, H (2005) A new method for the correlation of residual shear strength of the soil with mineralogical composition. J. Geotech. Geoenviron. Eng. 131(9), 1139-1150.

Tong, F, & Yin, J-H (2011) Nonlinear creep and swelling behavior of bentonite mixed with different sand contents under oedometric condition. Mar. Georesources Geotechnol. 29(4), 346-363.

Tovey, N (1986) Microanalyses of a Hong Kong marine clay. Geotech. Eng. 17(2), 167-210.

Verbrugge, J-C, & Schroeder, C (2018) *Geotechnical correlations for soils and rocks*: John Wiley & Sons.

Watabe, Y, Yamada, K, & Saitoh, K (2011) Hydraulic conductivity and compressibility of mixtures of Nagoya clay with sand or bentonite. Géotechnique 61(3), 211-219.

Wroth, C, & Wood, D (1978) The correlation of index properties with some basic engineering properties of soils. Can. Geotech. J. 15(2), 137-145.

Yilmaz, I, & Marschalko, M (2014) The effect of different types of water on the swelling behaviour of expansive clays. Bull. Eng. Geol. Environ. 73(4), 1049-1062.

Yin, J-H (1999a) Non-linear creep of soils in oedometer tests. Géotechnique 49(5), 699-707.

Yin, J-H (1999b) Properties and behaviour of Hong Kong marine deposits with different clay contents. Can. Geotech. J. 36(6), 1085-1095.

Yin, J-H, Chen, Z-J, & Feng, W-Q (2022) A general simple method for calculating consolidation settlements of layered clayey soils with vertical drains under staged loadings. Acta Geotech., 1-28.

Yin, J-H, & Feng, W-Q (2017) A new simplified method and its verification for calculation of consolidation settlement of a clayey soil with creep. Can. Geotech. J. 54(3), 333-347.

Yin, J-H, & Graham (1989) Viscous–elastic–plastic modelling of one-dimensional time-dependent behaviour of clays. Can. Geotech. J. 26(2), 199-209.

Yin, J, Tang, Y, Geng, W, & Xu, G (2021) Coupled effects of initial water content and swelling history on compression behaviors of bentonite. Bull. Eng. Geol. Environ. 80(6), 4929-4941.

Yin, Z, Xu, Q, & Yu, C (2014) Elastic-viscoplastic modeling for natural soft clays considering nonlinear creep. Int. J. Geomech.

Zeng, L, Hong, Z, Liu, S, & Chen, F (2012) Variation law and quantitative evaluation of secondary consolidation behavior for remolded clays. Chin. J. Geotech. Eng. 34(8), 1496-1500.

Zhang, P, Yin, Z-Y, Jin, Y-F, Chan, T H, & Gao, F-P (2021) Intelligent modelling of clay compressibility using hybrid meta-heuristic and machine learning algorithms. Geosci. Front. 12(1), 441-452.

Zhu, J-G, & Yin, J-H (2000) Strain-rate-dependent stress-strain behavior of overconsolidated Hong Kong marine clay. Can. Geotech. J. 37(6), 1272-1282.

Zhu, Q-Y, Yin, Z-Y, Hicher, P-Y, & Shen, S-L (2016) Nonlinearity of one-dimensional creep characteristics of soft clays. Acta Geotech. 11(4), 887-900.

Zhuang, X, Wang, Q, & Zhu, H (2017) Effective properties of composites with periodic random packing of ellipsoids. MATL 10(2), 112.